Reply to Reviewer 1

Reviewer: Understanding the compound dry and hot events is very important to human being society and environments. This study proposes a new compound drought and heat index on daily scale, SCDHI, based on SAPEI and STI. This index is useful to quantify sub-monthly characteristics of compound dry and hot events. The topic is very interesting and suitable for HESS. I recommend the manuscript for acceptance with a minor revision. The detailed comments are provided below:

Author's reply: We highly appreciate the constructive comments and suggestions.

Reviewer (1): This study focuses the non-arid areas in China. Is SCDHI suitable for the arid areas?

Author's Reply (1): Thank you for your comment. In this study, we did not assess the application of SCDHI in arid areas in China, because of three reasons: (1) replenishment of water resources in the Chinese arid region is mainly from melted glacial or perennial frozen soil, and not from precipitation. The statistical drought indices are usually limited its role in revealing drought in such complex situation. (2) meteorological observations in Chinese arid regions are too scarce to conduct robust analysis (Wu et al., 2007; Xu et al., 2015). (3) From a practical perspective, calculating climate extreme indices across arid region with large-scale desert regions is less meaningless (Tomas-Burguera et al., 2020). Thus, we did not evaluate the application of SCDHI in arid region. In further study, we will try to develop the compound dry-hot index adopted arid regions.

We have added explanation in Lines 156-163.

Reference:

Tomas-Burguera, M., Vicente-Serrano, S. M., Peña-Angulo, D., Domínguez-Castro, F., Noguera, I., & El Kenawy, A. Global characterization of the varying responses of the Standardized Evapotranspiration Index (SPEI) to atmospheric evaporative demand (AED). Journal of Geophysical Research: Atmospheres, e2020JD033017.

Xu, K., Yang, D., Yang, H., Li, Z., Qin, Y., & Shen, Y. (2015). Spatio-temporal variation of drought in China during 1961–2012: A climatic perspective. Journal of Hydrology, 526, 253-264.

Wu, H., Svoboda, M. D., Hayes, M. J., Wilhite, D. A., & Wen, F. (2007). Appropriate application of the standardized precipitation index in arid locations and dry seasons. International Journal of Climatology: A Journal of the Royal Meteorological Society, 27(1), 65-79.

Reviewer (2): There was a similar index for characterizing CDHEs (Hao et al., 2020). I suggest the authors to discuss the difference between this study and the study of Hao et al. (2020), and highlight the novelty of this study in the Introduction section. Hao, Z., Hao, F., Singh, V. P., Ouyang, W., Zhang, X., & Zhang, S. (2020). A joint extreme index for compound droughts and hot extremes. Theoretical and Applied Climatology, 1-8.

Author's Reply (2): Thank you for your recommendation. The study of Hao et al. (2020) provides a good background for our study and partially inspired the idea to develop SCDHI.

We have added discussion in Lines 75-85.

Reviewer (3): Why is the growing season selected to identify CDHEs in Section 3.3? Please explain a little bit more on it.

Author's Reply (3): Thank you for your comment and suggestion. The compound dry-hot events were examined during the approximate growing season (April-September) because this is the time where they can cause major impacts. Duo to the strong seasonal cycle in temperature and precipitation and focusing on relative exceedance thresholds, mixing seasons could result in results that are difficult to interpret.

We have added explanation in Lines 528-529.

Reviewer (4): Abstract: the regional difference exists in the future change of the CDHE characteristics. The authors may want to add this in the abstract.

Author's Reply (4): Thank you for your suggestion. Indeed, there are difference between region for future change of the CDHE characteristics. Specifically, under RCP 8.5 scenario, CDHE in the central to west parts of China is expected to markedly increase by more than five times; duration in mid-west China potentially increases by approximately 1.5 times; severity over mid-west China is expected to more than triple under RCP 8.5.

We have added these contents in Abstract. Please see Lines 36-38.

Reviewer (5): P143: how reliable is interpolated data based on the kriging method? Did the author evaluate the interpolated 0.25-degree data?

Author's Reply (5): Thank you for your questions. A reliable interpolation method is important to provide fundamental data for research. To generate reliable gridded data in China, previous studies have compared different interpolation methods (e.g., ordinary nearest neighbor, local polynomial, radial basis function, inverse distance weighting, and ordinary kriging), and they found that the ordinary kriging method shows the best performance and yields higher interpolation accuracy than the other methods (Chen et al., 2010; Lin et al., 2002).

Datasets based on the kriging method have also been used extensively for drought analyses (Liu et al., 2016; Wu et al., 2013; Shen et al., 2019). Based on these previous research findings, the kriging method was thus used in this study, and we did not evaluate the kriging method but rely on previous findings.

We have added explanation in Lines 153-156.

Reference:

Chen, D., Ou, T., Gong, L., Xu, C. Y., Li, W., Ho, C. H., & Qian, W. (2010). Spatial interpolation of daily precipitation in China: 1951–2005. Advances in Atmospheric Sciences, 27(6), 1221-1232.

Lin, Z. H., Mo, X. G., Li, H. X., & Li, H. B. (2002). Comparison of three spatial interpolation methods for climate variables in China. Acta Geographica Sinica, 57(1), 47-56.

Liu, Z., Wang, Y., Shao, M., Jia, X., & Li, X. (2016). Spatiotemporal analysis of multiscalar drought characteristics across the Loess Plateau of China. Journal of Hydrology, 534, 281-299.

Shen, Z., Zhang, Q., Singh, V. P., Sun, P., Song, C., & Yu, H. (2019). Agricultural drought monitoring across Inner Mongolia, China: Model development, spatiotemporal patterns and impacts. Journal of Hydrology, 571, 793-804.

Wu, J., Zhou, L., Liu, M., Zhang, J., Leng, S., & Diao, C. (2013). Establishing and assessing the Integrated Surface Drought Index (ISDI) for agricultural drought monitoring in mid-eastern China. International Journal of Applied Earth Observation and Geoinformation, 23, 397-410.

Reviewer (6): P152: what is the standard number of GB/T 20481-2017? It would be clearer if the authors add some more information on it.

Author's reply (6): Thank you for your question and suggestion. The PDSI is a semi physical drought index based on the land surface water balance. The parameters of the standardized procedure of the conventional PDSI, including the climatic characteristic and duration factors, are empirically derived using the meteorological data of the central USA with its semi-arid climate. Therefore, the portability and spatial comparability of the conventional PDSI are relatively poor in other regions of the world. To develop a PDSI suited for China, the PDSI calculation procedure was revised based on long-term meteorological data of several in-situ stations distributed around China that represent the climate characteristic of mainland China. A China national standard of classification of meteorological drought with standard number of GB/T 20481–2017 provides the corrected calculation procedure of the PDSI specific for China:

$$Z_i = K_m d_i \tag{1}$$

$$K_m = \left(\frac{16.84}{\sum_{j=1}^{12} \overline{D}_j K'_m} \right) K'_m \tag{2}$$

$$K'_m = 1.6\log_{10}\left[\left(\frac{\overline{PE}_m + \overline{R}_m + \overline{RO}_m}{\overline{P}_m + \overline{L}_m} + 2.8\right) / \overline{D}_m\right] + 0.4 \tag{3}$$

$$X_i = 0.755 X_{i-i} + Z_i / 1.63 \tag{4}$$

We have added the calculation procedure of PDSI of the GB/T 20481–2017 in supplementary material.

Reviewer (7): P155: soil moisture data in different depths is available in the GLDAS product. Why did the authors choose the root zone soil moisture to evaluate the drought indices? How about soil moisture in the surface layer and in total column?

Author's reply (7): Thank you for your questions and comments. Some soil moisture datasets in the GLDAS product provides different depths. For instance, the NOAH model of GLDAS has total of 4 layers thickness: 0-10, 10-40, 40-100, and 100-200 cm, while NOAH only has monthly temporal resolution. The CLSM product used in this study does not have explicit vertical levels, instead soil moisture is represented in Surface (0-2cm), and Root Zone (0-100cm). Root zone soil moisture is chosen over the surface soil moisture on account of its appositeness to characterize drought and low noise relative to surface soil moisture (Hunt et al., 2009; Osman et al., 2020). For drought monitoring, this product has the advantage of offering spatially and temporally complete root zone soil moisture estimates on a grid. Furthermore, standard drought indices based on a time scale of three months (or higher) seem to more representative of drought behavior in deeper soil layers (Fig. 6 in Nicolai-Shaw et al., 2017).

We have added illustration in Lines 177-181.

Reference:

Hunt, E. D., Hubbard, K. G., Wilhite, D. A., Arkebauer, T. J., & Dutcher, A. L. (2009). The development and evaluation of a soil moisture index. International Journal of Climatology, 29(5), 747-759.

Nicolai-Shaw, N., J. Zscheischler, M. Hirschi, L. Gudmundsson, and S. I. Seneviratne (2017). A drought event composite analysis using satellite remote-sensing based soil moisture. Remote Sensing of Environment 203, 216-225.

Osman, M., Zaitchik, B. F., Badr, H. S., Christian, J. I., Tadesse, T., Otkin, J. A., & Anderson, M. C. (2020). Flash drought onset over the Contiguous United States: Sensitivity of inventories and trends to quantitative definitions. Hydrology and Earth System Sciences Discussions, 1-21.

Reviewer (8): P163: the resolutions of eight climate models are different. Are the results from these models resampled to the same resolution?

Author's reply (8): Thank you for your question. We are sorry that we did not provide a clear description of how the data was processed.

Earth system models (ESMs) provide useful information of future climate projections through global-scale simulations. However, the coarse resolution of ESMs restricts their usefulness for many sub-region-scale applications, requiring downscaling of climate model output (Chen et al., 2019; Fenta and Disse, 2018). In this study, the bias-corrected climate imprint method (Werner and Cannon, 2016), a statistical downscaling method based on the delta approach, was applied to downscale the climate model output to a spatial resolution of 0.25°.

We have added illustration in Lines 203-205.

Reference:

Werner, A. T., & Cannon, A. J. (2016). Hydrologic extremes–an intercomparison of multiple gridded statistical downscaling methods. Hydrology and Earth System Sciences, 20(4), 1483.

Reviewer (9): P164: five is missing after phase.

Author's reply (9): Thank you for your comment. We have done.

Reviewer (10): P448: what does the national weather reports look like? I did not see the information on the two CDHEs from the national weather reports.

Author's reply (10): Thank you for your question. The national weather report is a public service product provided by China Meteorological Administration (http://www.weather.com.cn/). Specifically, the CDHE in Sichuan-Chongqing region during summer of 2006 is reported in http://www.weather.com.cn/zt/kpzt, while the other event during July to September of 2009 was recorded in Yearbook of Meteorological Disasters in China 2010.

We have added illustration Lines 520-521.

Reviewer (11): Figs. 3 and 5: is soil moisture is represented by the standardized anomaly? If yes, please briefly describe this. And what is the solid black line all the way from the beginning time down to the ending time?

Author's reply (11): Thank you for your questions and suggestions. The soil moisture in Figure 3 and 5 represents the standardized anomaly. To avoid the effect of seasonality, the soil moisture was fitted by Gamma probability distribution, and then was standardized by normal quantile transformation. The value of solid black line is at -0.5, indicating the distinction between drought and non-drought according to our definition.

We have added illustrations in Lines 185-187 and Figure 3 and 5:

Reviewer (12): Figs. 4, 6, and 10: please add the longitude and latitude on the figures.

Author's reply (12): Thank you for your comment. We have added the longitude and latitude on the figures. Please see Figure 4, 6, 8, and 9.

Reviewer (13): Fig. 8: I cannot see the difference among three panels in the last line. Is it because an inappropriate colobar is used?

Author's reply (13): Thank you for your comment. We have revised the figure. Please see Figure 7.

Reviewer (14): Figure 11d): the numbers 1.8 and 2 in the colorbar are placed wrongly. They should be exchanged.

Author's reply (14): Thank you for your comment. We are sorry for the mistake and will check throughout the manuscript to avoid similar mistakes. We have revised the figure. Please see Figure 10.

Reviewer (15): Figs. 12 and 13: is the historical period used here 1961-2005 or 1951-2018? The authors mentioned that they obtained the model outputs for the 1961-2005 period in Section 2.1. However, the 1961-2005 period does not show up in the results. And is the historical data from the CMIP5 climate models or from the interpolated observations? If the observational data is used as the reference, how the authors resolve the resolution difference between the observational data and the model results?

Author's reply (15): Thank you for your comments and question. In Figure 12 and 13 of the first-round manuscript, the historical periods are from 1961 to 2018, and the observational datasets were used. To match the spatial scale, the bias-corrected climate imprint method, was applied to bias correct and downscale the model output to same resolution in this study (see Author's reply (8)).

Reference:

Werner, A. T., & Cannon, A. J. (2016). Hydrologic extremes–an intercomparison of multiple gridded statistical downscaling methods. Hydrology and Earth System Sciences, 20(4), 1483.

Reviewer (16): Please check through the manuscript and correct all the grammar mistakes.

Author's reply (16): Thank you. We have checked the revision thoroughly for grammar mistakes.

Reply to Reviewer 2

Reviewer: Interesting objective, interesting method, but hard to read.

Author’s reply: Thank you for your comments and suggestions.

Reviewer (1): (a) The paper discusses a standardized index for assessing compound dry and hot conditions. Overall, I find the paper not in a really good shape, and I have to admit that I found it really hard to read due to the excessive amount of acronyms. The paper is so technical that for a reader who does know something about the topic, it is still very hard to follow. (b) For me it did not became entirely clear what are now the new insights that can be learned by creating this new index that were not known before. (c) I also think that the authors should make a new selection of figures and reduce the paper to the essentials, because with the figures in the text and the supplementary material there are so many panels showing China that it becomes overwhelming to the reader. I put some comments below that could help in improving the paper.

Author’s reply: Thank you for your comments and suggestions.

(a) We are sorry for the excessive number of acronyms. We have strongly reduced the utilization of the abbreviations in revised manuscript.

(b) Please allow us to clarify the new insights of this index:

Much effort has been made to study the compound dry-hot event in recent years. Utilizing thresholds to define the concurrent events, the frequency of compound events has received much attention (Wu et al., 2019; Zhang et al., 2019). However, this approach fails to measure compound event characteristics (e.g., duration, severity, and intensity), and is inconvenient for comparing compound event characteristics through different climates (Wu et al., 2020). Several indices were thus proposed for analyzing the characteristics of the compound events, such as standardized compound event indicator and standardized compound dry-hot index. These indices provide useful tools to understanding compound dry-hot event characteristics. However, they are subject to some shortcomings including the fixed monthly scale and the disregard of evapotranspiration, which may limit their use in monitoring the detailed evolution of compound dry and hot events.

In addition, severe concurrent drought and heat can suddenly strike a region within short duration when extreme weather anomalies persist over the same region (Röthlisberger and Martius, 2019; Wang et al., 2016). Concurrent short-term drought and heatwaves can pose great socio-economic risks (Zhang et al., 2019). There is thus a need to have readily available indices capable of monitoring sub-monthly compound dry-hot conditions. A suite of indices have been proposed for the assessments of droughts and heatwaves separately, yet there is no index available for incorporating the joint variability of dry and hot conditions at sub-monthly scale.

The proposed SCDHI index provides a new tool to monitor and quantify the characteristics of compound dry-hot events at multiple time scale (e.g., daily, weekly and monthly) to provide detailed information on their initiation, development, termination, and trends.

We have rewritten the motivation and benefits of this new index in Lines 127-142.

(c) We agree that the figures in the first-round manuscript need to be reduced. Specifically, as the results on 3, 6, 9, 12-month scale SAPEI/SCDHI in Figure 2, 4, 6, 8, 9, 10 are generally similar, we have only shown results on 3-month scale SAPEI/ SCDHI, and removed the similar results on other time scales in these Figures. In addition, we have removed the Figure 7 and 13 in revised manuscript.

The supplementary materials mainly involve the metrics for selecting copula, and assessment of SAPEI/SCDHI ability to monitor monthly drought/compound dry-hot conditions using real-world typical events. These analyses are necessary but not essential, so placing them in the supplementary material without adding manuscript space. We have reduced the text content related to supplementary materials, and subfigures in supplementary materials, but kept essential figure and content to ensure the integrity of paper structure.

Reference:

Röthlisberger, M. and Martius, O.: Quantifying the Local Effect of Northern Hemisphere Atmospheric Blocks on the Persistence of Summer Hot and Dry Spells, Geophys. Res. Lett., doi:10.1029/2019GL083745, 2019.

Wang, L., Yuan, X., Xie, Z., Wu, P. and Li, Y.: Increasing flash droughts over China during the recent global warming hiatus, Sci. Rep., doi:10.1038/srep30571, 2016.

Wu, X., Hao, Z., Hao, F. and Zhang, X.: Variations of compound precipitation and temperature extremes in China during 1961–2014, Sci. Total Environ., 663, 731–737, doi:10.1016/j.scitotenv.2019.01.366, 2019.

Wu, X., Hao, Z., Zhang, X., Li, C. and Hao, F.: Evaluation of severity changes of compound dry and hot events in China based on a multivariate multi-index approach, J. Hydrol., 583, 124580, doi:10.1016/j.jhydrol.2020.124580, 2020.

Zhang, Y., You, Q., Mao, G., Chen, C. and Ye, Z.: Short-term concurrent drought and heatwave frequency with 1.5 and 2.0 °C global warming in humid subtropical basins: a case study in the Gan River Basin, China, Clim. Dyn., 52(7–8), 4621–4641, doi:10.1007/s00382-018-4398-6, 2019.

Reviewer (2): It could be good to mention already in the title that this study only concerns China. The paper does not deliver a universal index for compound dry and hot conditions, but one that is only developed for application in China.

Author's reply (2): Thank you for your comments and suggestions. Because developing a sub-monthly index requires datasets with high temporal resolution (e.g., daily precipitation, maximum air temperature, mean air temperature, minimum air temperature, relatively humidity, wind speed, and sunshine duration), it is difficult to collect all these daily datasets on a global scale. While the index is computed for China base on readily available datasets, the methodology is universal.

China has vast territory and complex and diverse climates, and during the past decades, it suffers from frequent and severe compound dry-hot events (Wu et al., 2019). Overall, it serves as an excellent setting to study compound dry-hot events.

We have changed the title into: "A standardized index for assessing sub-monthly compound dry and hot conditions: application in China"

Reference:

Wu, X., Hao, Z., Zhang, X., Li, C., & Hao, F. (2019). Evaluation of severity changes of compound dry and hot events in China based on a multivariate multi-index approach. Journal of Hydrology, 583, 124580.

Reviewer (3): As a reviewer, it did not become completely clear to me what the exact problem is of combined dry and hot conditions. There are many examples, but their explanation does not really get to the core: why do we need an indicator for dry and hot? Please improve this in the revision.

Author's reply (3): Thank you. Different combinations of dry and hot conditions lead to different types of impacts including crop failure vegetation impacts or wild fires. Thereby it matters hot and dry it really is. Slightly hotter conditions may exacerbate impacts from dry conditions (Ribeiro et al., 2020). Furthermore, the correlation between hot and dry conditions render a naive combination of univariate indicators of hot and dry events unsuitable for estimating combined impacts. A combined dry-hot indicator implicitly accounts for the dependence between hot and dry conditions and provides a univariate metric to measure the intensity of combined stress due to heat and drought. For crops it has been shown that such a bivariate indicator can explain crop yield better than typically used linear regression models (Zscheischler et al., 2017).

The author's reply (1) has provided further motivation for such an index. We have reduced the number of given examples, and written the introduction. Please see Lines 46-142.

Reference:

Ribeiro, A. F. S., Russo, A., Gouveia, C. M., Páscoa, P., and Zscheischler, J.: Risk of crop failure due to compound dry and hot extremes estimated with nested copulas, Biogeosciences Discuss., in review, 2020.

Zscheischler, J., Orth, R., and Seneviratne, S. I.: Bivariate return periods of temperature and precipitation explain a large fraction of European crop yields, Biogeosciences, 14, 3309–3320, 2017.

Reviewer (4): I find the methods a little ill-described. There are many references back to previous papers, but please list the equations of the equations that you take from these papers, because now the reader has to look up essential information in previous papers. Also, please be exact what the source of the input data is that is needed to compute all the variables that you need.

Author's reply (4): Thank you for your comments and suggestions. We are sorry for the unclear description on methods. In this study, only the SAPEI involve the previous papers, and the manuscript have already shown the equations that were used to calculate this index, i.e., equation (1).

The SCDHI calculation relies on STI and SAPEI. STI is calculated from maximum temperature, while SAPEI is calculated from precipitation and potential evapotranspiration. The Penman-Monteith method is used to calculate the potential evapotranspiration, requiring maximum air temperature, mean air temperature, minimum air temperature, relatively humidity, wind speed, and sunshine duration.

We have added illustration in Lines 214-216.

Reviewer (5): Line 203: how does one use a probability distribution to create daily time series, and against what is it fitted? I do not understand the procedure.

Author's reply (5): Thank you for your question. The probability is not used to create daily time series, but applied to fit a time series.

Please allow us to show a case for SAPEI calculation:

Taking the calculation of SAPEI on May 1 of each year (1961-2018) as an example, with respect to 3-month scale SAPEI, the total water surplus or deficit in three months before May 1 of each year is calculated to represent the dry and wet condition on May 1, and thus, there are 58 values representing the dry and wet conditions on May 1 of each year from 1961 to 2018. The water surplus or deficit was calculated through the difference between precipitation and potential evapotranspiration. For calculating a standardized index, a probability distribution was used to fit the daily time series (58 values), which was then transformed into a standard normal distribution (resulting in the SAPEI) using the classical approach of Barton et al. (1965).

We have added a case of SAPEI calculation in supplementary materials.

Reference:

Barton, D. E., Abramovitz, M. and Stegun, I. A.: Handbook of Mathematical Functions with Formulas, Graphs and Mathematical Tables., J. R. Stat. Soc. Ser. A, doi:10.2307/2343473, 1965.

Reviewer (6): Line 219: what is copula theory?

Author's reply (6): Thank you for your question.

Developed by Sklar (1959), copulas are functions that link univariate distribution functions to form multivariate distribution functions. The merit of using copulas to construct multivariate distributions is that copulas can separate the dependence effects from the marginal distribution effects. Construction of multivariate distribution is thus reduced to studying the relations among the correlated random variables if marginal distributions are given.

Considering a situation with two random variables, Sklar's Theorem states that if $F_{X,Y}(x, y)$ is a two-dimensional distribution function with marginal distributions $F_X(x)$

and $F_Y(y)$, then there exists a copula C such that:

$$F_{X,Y}(x,y) = C(F_X(x), F_Y(y)) \quad (1)$$

Conversely, for any univariate distributions $F_X(x)$ and $F_Y(y)$ and any copula C, the function $F_{X,Y}(x,y)$ defined above is a two-dimensional distribution function with marginal distributions $F_X(x)$ and $F_Y(y)$. Furthermore, if $F_X(x)$ and $F_Y(y)$ are continuous, then C is unique.

Under the assumption that the marginal distributions are continuous with probability density functions $f_X(x)$ and $f_Y(y)$, the joint probability density function then becomes

$$f_{X,Y}(x,y) = c(F_X(x), F_Y(y)) f_X(x) f_Y(y) \quad (2)$$

Where c is the density function of C.

Books of Nelsen (2006) introduce a copula theory in detail.

We have added a brief introduction of copula theory in supplementary materials.

Reference:

Sklar, K.: Fonctions de repartition a n Dimensions et Leura Marges, Publ. Inst. Stat. Univ. Paris, 8, 229–231, 1959

Reviewer (7): Lines 226-250: This could use some explanatory figures. It is nearly impossible to understand for a reader that is not familiar with the specialized methods that are used here.

Author's reply (7): Thank you for your comment and suggestion. Figure S4 in supplementary material have already illustrated the SCDHI development.

Reviewer (8): Line 265: I think that there are more appropate and far older references for the definition of the POD and FAR.

Author's reply (8): Thank you for your suggestion. We have added the reference:

"Winston, H.A., Ruthi, L.J.: Evaluation of RADAP II severe-storm-detection algorithms. Bull. Am. Meteorol. Soc., 67(2), 145-150, 1986."

Reviewer (9): Section 3.1: What is the added value from SAPEI compared to much simpler metrics as soil moisture, or if that is not available P-E, or an simple estimation of evapotranspiration?

Author's reply (9): That is a good question and is basically related to the lack of availability of soil moisture data.

Soil moisture would be the most appropriate variable for agriculture drought monitoring and analyses (Mishra and Singh, 2010). However, there are few long-term and large-scale observational soil moisture datasets due to insufficient observation stations around the world, especially for developing regions, which limits it wide use in drought monitoring and analyses. Thus, using observational hydrometeorological datasets, the complex physical process models, such as the Community Land Model, are widely used to simulate the soil moisture. However, running such models requires highly trained personnel not usually available at local agencies. In addition, when the model is used locally, it generally needs to be calibrated and verified by observational soil moisture and other hydrometeorological datasets. This certainly limits the wide use of soil moisture as a drought indicator.

An evapotranspiration-based drought index provides a useful tool for drought monitoring and analyses. However, in many regions and operational settings, evapotranspiration is derived from potential evapotranspiration (PET) through parameterizations of soil-water and plant-water availabilities that are of questionable value on operational space and time scales: in such cases PET may serve as an independent drought indicator (Hobbins et al., 2016). Recently, the evaporative demand drought index (EDDI) based solely on the PET is used to analyze and monitor flash droughts (McEvoy et al., 2016). However, EDDI only considers for PET and thus is inappropriate for regions with non-constraining soil moisture conditions, e.g. humid regions, given that positive PET anomaly is not representative of actual drought conditions (Vicente-Serrano et al., 2018).

The SAPEI relies on the precipitation and potential evapotranspiration. There are generally available observational precipitation and datasets for calculating potential evapotranspiration in most countries around the world. Therefore, SAPEI can be directly calculated using observed meteorological datasets, and the calculation process is simple. In addition, it has multiple time scales, and the long-time scale SAPEI is sensitive to soil moisture variation. It is commonly accepted that drought is a multiscalar phenomenon. The time scale over which water deficits accumulate becomes extremely important, and it functionally separates hydrological, agricultural, and other droughts. Drought indices must be associated with a specific time scale to be useful for monitoring and managing different usable water resources (Vicente-Serrano et al., 2010). Overall, the SAPEI meets the requirements of a drought index, given the fact that it shows reliable and robust ability for drought analysis and monitoring. Like the SPEI and SPI, SAPEI includes multiple time scales (3-, 6-, 9-, and 12- month) to monitor droughts at monthly resolution. However, SAPEI has the advantage over SPEI regarding sub-monthly drought monitoring. Such an index could help fill a gap between science and applications in that it would be operationally tractable for detecting and monitoring both short-term and sustained droughts.

We have added discussion on the added value of SAPEI compared with soil moisture indices in Lines 421-432.

Reference:

Mishra, A. K., & Singh, V. P. (2010). A review of drought concepts. Journal of hydrology, 391(1-2), 202-216.

Hobbins, M. T., Wood, A., McEvoy, D. J., Huntington, J. L., Morton, C., Anderson, M., & Hain, C. (2016). The evaporative demand drought index. Part I: Linking drought evolution to variations in evaporative demand. Journal of Hydrometeorology, 17(6), 1745-1761.

McEvoy, D. J., Huntington, J. L., Hobbins, M. T., Wood, A., Morton, C., Anderson, M., & Hain, C. (2016). The evaporative demand drought index. Part II: CONUS-wide assessment against common drought indicators. Journal of Hydrometeorology, 17(6), 1763-1779.

Vicente-Serrano, S. M., Beguería, S., López-Moreno, J. I., Angulo, M., & El Kenawy, A. (2010). A new global 0.5 gridded dataset (1901–2006) of a multiscalar drought index: comparison with current drought index datasets based on the Palmer Drought Severity Index. Journal of Hydrometeorology, 11(4), 1033-1043.

Vicente-Serrano, S. M., Miralles, D. G., Domínguez-Castro, F., Azorin-Molina, C., El Kenawy, A., McVicar, T. R., ... & Peña-Gallardo, M. (2018). Global assessment of the Standardized Evapotranspiration Deficit Index (SEDI) for drought analysis and monitoring. Journal of Climate, 31(14), 5371-5393.

Reviewer (10): There are too many references to the supplementary material throughout the text. I suggest the authors reevaluate the necessity for each of the figures and come up with a set that is crucial to the story. This is not a research letter, there is more than enough space.

Author's reply (10): Thank you for your comments and suggestions. The supplementary materials mainly involve the metrics for selecting copula, and assessment of SAPEI/SCDHI ability to monitor monthly drought/compound dry-hot conditions using real-world typical events. These analyses are necessary but not essential, so placing them in the supplementary material without adding manuscript space. If we remove these materials, the ability of the two indices to monitor monthly drought/dry-hot conditions could not be verified.

So, we would like to keep them, but have selected the essential panels and reduced the content related to supplementary materials. Please see Lines 348-361 and 376-387.

Reviewer (11): Line 462. If a hot index is based on absolute temperature, it seems trivial that places that are closer to the equator at low altitudes have the largest probability of a hot event. Can you explain more about the location where the outcome surprised you, or where new insights were found?

Author’s reply (11): Thank you for your comment and suggestion.

In this study, the STI representing the hot condition is calculated by the temperature variation within a specific grid point (similar to common drought indices). For example, with respect to one certain grid point, the 1 January STI are computed on the 1 January temperature datasets observed during 1961-2018 at each grid point. In other words, the hot index (STI) is not affected by regional location and are only related to its changes within the grid point. Hot events are always only hot relative to the local climatology.

In addition, the Figure 11 shows the characteristics (e.g., frequency) of the compound dry-hot events. Though the compound dry-hot event is closely related to the extreme temperature, it reflects the concurrent dry and hot conditions. Extreme temperature is more frequent in some regions, but there may be relatively less compound dry-hot events due to less droughts.

In this study, we found that a high frequency of compound events was detected in southern China, and the events generally lasted about 25 days (Fig. 11a). The occurrence of extreme climate (e.g. high temperature, low humidity, and sunny skies) can appear within a short period without resulting in long-lasting compound events, but rather, short-term droughts and heatwave lasting a few weeks (Mo and Lettenmaier, 2015; Zhang et al., 2019). Previous studies state that short-term dry and hot events occur more frequently in southern regions than in other parts of China (Otkin et al., 2018; Wang et al., 2016). South China is a humid region where evapotranspiration is mainly controlled by energy supply because soil moisture is usually sufficient. The evaporation demand could increase significantly during a short period when strong, transient meteorological changes occur. Through influencing evapotranspiration variation, short-term meteorological variables (e.g., solar radiation and sunshine duration) are considered an important factor in drought and hot concurrences. For instance, the largely increase in sunshine duration due to clear sky create excessive evapotranspiration, which in turn decrease soil moisture. More surface sensible heat fluxes are transferred to the near-surface atmosphere to further increase air temperatures and makes precipitation rare These land-atmosphere interactions altogether create favorable conditions for concurrent drought and hot. Therefore, concurrent dry-hot events are likely to occur in south China.

We have added discussion on why southern China experience more compound dry-hot events. Please see Lines 549-562.

Reference:

Mo, K. C., & Lettenmaier, D. P. (2015). Heat wave flash droughts in decline. Geophysical Research Letters, 42(8), 2823-2829.

Otkin, J. A., Svoboda, M., Hunt, E. D., Ford, T. W., Anderson, M. C., Hain, C., & Basara, J. B. (2018). Flash droughts: A review and assessment of the challenges imposed by rapid-onset droughts in the United States. Bulletin of the American Meteorological Society, 99(5), 911-919.

Wang, L., Yuan, X., Xie, Z., Wu, P., & Li, Y. (2016). Increasing flash droughts over China during the recent global warming hiatus. Scientific reports, 6, 30571.

Zhang, Y., You, Q., Mao, G., Chen, C., & Ye, Z. (2019). Short-term concurrent drought and heatwave frequency with 1.5 and 2.0 C global warming in humid subtropical basins: a case study in the Gan River Basin, China. Climate dynamics, 52(7-8), 4621-4641.

Reviewer (12): Lines 485 and further: (a) How are the RCP scenarios computed in your index? This does not seem trivial to me, how is the input acquired? (b) It would be nice to know which of the observed increases in due to temperature alone and which due to more complex interactions?

Author’s reply (12): Thank you for your questions and suggestion.

(a) To obtain the future climate scenarios data, we collect eight global climate models, including CanESM2, CNRM-CM5, CSIRO-Mk3.6, MIROC-ESM, MPI-ESM-LR, BCC-CSM1-1, IPSL-CM5A-LR, and MRI-CGCM3, to project the future climate conditions. These global climate models exhibit good performance to simulate the key features of precipitation and temperature in China. We obtained climate variables (i.e., precipitation, temperature, relatively humidity, wind speed, and shortwave and longwave radiations) for the future periods for the three Representative Concentration Pathways (RCPs) including RCP 2.6 (low emission scenario), RCP 4.5 (moderate emission scenario) and RCP 8.5 (high emission scenario). The bias-corrected climate imprint method, one of the delta statistical downscaling methods, was applied to downscale the climate model output to same resolution as the observations. Using the downscaling datasets, the SCDHI was computed, and was used to analyze future compound dry-hot events.

We have clarified these points in Lines 203-206.

(b) That is a good suggestion. We have calculated the future SCDHI considering only temperature change, and then this SCDHI will compared to historical reference. Finally, this result has been compared with the Figure 12 in first-round manuscript to illustrate future changes in characteristics of the compound dry and hot events due to temperature change.

The detailed analyses are shown in Lines 596-622 and Figure 12 in revised manuscript.

A standardized index for assessing sub-monthly compound dry and hot conditions: application in China

Jun Li[1], Zhaoli Wang[1,2], Xushu Wu[1,2,*], Jakob Zscheischler[3,4,5], Shenglian ~~Guo[5]~~Guo[6], Xiaohong ~~Chen[6]~~Chen[7]

[1] *School of Civil Engineering and Transportation, State Key Laboratory of Subtropical Building Science, South China University of Technology, Guangzhou 510641, China.*

[2] *Guangdong Engineering Technology Research Center of Safety and Greenization for Water Conservancy Project, Guangzhou 510641, China.*

[3] *Climate and Environmental Physics, University of Bern, Sidlerstrasse 5, 3012 Bern, Switzerland.*

[4] *Oeschger Centre for Climate Change Research, University of Bern, Bern, Switzerland.*

[5] *Department of Computational Hydrosystems, Helmholtz Centre for Environmental Research - UFZ, Leipzig, Germany*

~~[5]~~[6] *State Key Laboratory of Water Resources and Hydropower Engineering Science, Wuhan University, Wuhan 430072, China.*

~~[6]~~[7] *Center for Water Resource and Environment, Sun Yat-Sen University, Guangzhou 510275, China*

∗*Correspondence: xshwu@scut.edu.cn.*

Abstract: Compound dry~~ and ~~-hot conditions pose large impacts on ecosystems and society worldwide. A suite of indices are proposed for the assessments of droughts and heatwaves previously, yet there is no index available for incorporating the joint variability of dry and hot conditions at sub-monthly scale. Here, we introduce a daily-scale index, termed as the standardized compound drought and heat index (SCDHI), to measure the intensity of compound dry and hot conditions. SCDHI is based on the daily drought index (the standardized antecedent precipitation evapotranspiration index (SAPEI)) and the ~~Standardized ~~standardized ~~Temperature ~~temperature ~~Index ~~index (STI) and a joint probability distribution method. The new index is verified against real-world compound dry and hot events and the related observed vegetation impacts in China. SCDHI can not only monitor the long-term compound dry and hot events, but also capture such events at sub-monthly scale and reflect the related vegetation activity impacts. The identified compound events generally persisted for 25-35 days and the southern China suffered from compound events most frequently. In future, the frequency, duration, severity and intensity of compound events increase throughout China in response to anthropogenic climate change, of which the frequency would generally increase by 1-3 times and the duration and severity increase by 50%; under largest emission scenario, duration, severity, and frequency across Midwest China increase by at least 3 times. ~~, independent of the emission scenarios.~~ The new index can provide a new tool to quantify sub-monthly characteristics of compound dry and hot events, conducive to the timely monitoring of their initiation, development, and decay which are vital for decision-makers and stake-holders to release early and timely warnings.

Keywords: compound event; SCDHI; SAPEI; sub-monthly scale; China

1 Introduction

Compound dry~~ and ~~-hot event~~ (CDHE)~~ have been observed for all continents in recent decades (Hao et al., 2019; Mazdiyasni and AghaKouchak, 2015; Manning et al., 2019; Sutanto et al., 2020). The frequent ~~CDHEs ~~compound dry-hot events have led to more devastating impacts on natural ecosystems and human society than individual events (Zscheischler et al., 2014, 2018; Chen et al., 2019; Hao et al., 2018a).~~ For example, Russia was simultaneously struck by an unprecedented drought and hot in the summer of 2010, which caused large-scale crop failures, wildfires, and human mortality (Zscheischler et al., 2018).~~ Unfortunately, the extreme droughts and hots are expected to occur more frequently in the coming decades under global warming, which potentially results in more compound events in many parts of the world, especially for wet and humid regions (Wu et al., 2020; Swain et al., 2018, Zscheischler and Seneviratne, 2017a). Therefore, understanding such events are of crucial importance to provide the most fundamental information to help disaster mitigation.

Much effort has been made to study the compound events in recent years. Utilizing different thresholds to define the concurrent climate extremes for a specific period, the frequency of compound events has ~~received a~~received a great deal of attention (Wu et al., 2019; Zhang et al., 2019). Although this approach can~~ can~~ detect compound event occurrence, it fails to quantitatively measure compound event characteristics such as duration, severity, and intensity, and is inconvenient for comparison of compound event characteristics through different climates (Wu et al., 2020). Therefore, to overcome these shortages, several joint climate extreme indices have been proposed for analyzing the characteristics of the compound events. ~~For example, the climate extreme index integrated by temperature and soil moisture extremes was presented for monitoring trends in multiple types of climate extremes across large regions, and has been~~

~~employed to assess changes in spatial extent (Gallant et al., 2014). In recent years, several compound dry and hot indices have been developed. For example, t~~Specifically, the ~~Standardized~~ standardized ~~Dry~~ dry and ~~Hot~~ hot ~~Index~~ index based on the ratio of the marginal probability distribution functions of precipitation and temperature was proposed to measure the extreme degree of a compound drought and hot extreme event (Hao et al., 2018). Hao et al. (2019, 2020) recently proposed the ~~Standardized~~ standardized ~~Compound~~ compound ~~Event~~ event ~~Indicator~~ indicator ~~(SCEI)~~ and compound dry-hot index to assess the severity of compound dry and hot events by jointing the marginal distribution of ~~Standardized~~ standardized ~~Precipitation~~ precipitation ~~Index~~ index (SPI) and ~~Standardized~~ standardized ~~Temperature~~ temperature ~~Index~~ index (STI) using the copula theory. These two joint indices provide useful tools to improve our understanding of the frequency, spatial extent and severity of the compound dry-hot event. However, they are inevitably subjected to some shortcomings including the fixed monthly scale and the disregard of evapotranspiration, which may limit their use in monitoring the detailed evolution of compound dry and hot events.

With the occurrence of extreme climate (e.g. high temperature, low humidity, and sunny skies), droughts can evolve rapidly (~~Chen et al., 2019;~~ Koster et al., 2019; ~~Mo and Lettenmaier, 2015;~~ Otkin et al., 2018; Yuan et al., 2019; Li et al., 2020a). Such extreme weather can appear within a short period without resulting in long-lasting compound events, but rather, short-term droughts and heatwaves lasting a few weeks or even days (Mo and Lettenmaier, 2016; Zhang et al., ~~2017~~2019). Severe concurrent drought and heat can suddenly strike a region with a relatively short duration when extreme weather anomalies persist over the same region (Röthlisberger and Martius, 2019; Wang et al., 2016). Concurrent short-term drought and hot can pose greater potential socio-economic risks because the combination of these events can exacerbate their respective environmental and societal impacts (Kirono et al., 2017; Schumacher et al., 2019; Sedlmeier et al., 2018). Specifically, even short-term concurrent dry and hot extremes can lead to significant agricultural loss if they occur within sensitive stages in crop development such as emergence, pollination, and grain filling (Zhang et al., 2019). ~~For example, a strong precipitation deficit along with record high temperatures have led to severe impacts during May and early June in 2012 across the central U.S. (Ford and Labosier, 2017; Otkin et al., 2013). Such short-term concurrent dry and hot events regularly inflict widespread agricultural crop losses and drastically cut down livestock population, making it one of the most costly natural hazards in the U.S. history at tens of billions of economic losses (Anderson et al., 2016; Otkin et al., 2019)~~. Under climate change, short-term concurrent dry and hot extremes are expected to increase (especially for humid regions), potentially causing substantial damage to natural ecosystems and society (Li et al., 2020b; Sun et al., 2019). To improve understanding of such short-term compound events and make early and timely warnings, decision-makers and stakeholders require more detailed information such as the start time, severity, and the projected tendency in the coming days rather than the average state at a fixed monthly scale. Correspondingly, sub-monthly scale indices for characterizing short-term compound dry and hot events are needed. In addition, t~~T~~hrough the influence of evapotranspiration, short-term meteorological variables (e.g., temperature and radiation ~~solar radiation and sunshine duration~~) are considered an important factor in drought and heatwave concurrences (James et al., 2010). ~~For example, the largely increase in sunshine duration due to clear sky creates excessive evapotranspiration, which in turn decreases soil moisture (Ford et al., 2015). More surface sensible heat fluxes is transferred to the near-surface atmosphere to further increase air temperatures~~

~~and prohibit precipitation (Miralles et al., 2019; Vogel et al., 2018). Together, these land-atmosphere interactions create favorable conditions for concurrent drought and heatwaves (Mo and Lettenmaier, 2016; Otkin et al., 2018).~~ Thus, the development of a compound drought and heat index should consider other important drought/hot-related factors including temperature and precipitation~~including temperature and precipitation~~ (e.g. evapotranspiration).

The complexity of compound events makes it an unusual task to develop a simple and robust index to quantify their past and future changes (Zscheischler et al., 2020). A suite of indices are proposed for the assessments of droughts and heatwaves previously, yet there is no index available for incorporating the joint variability of dry and hot conditions at sub-monthly scale. Here we aim to formulate a compound drought and heat index, called the standardized compound drought and heat index (SCDHI), for monitoring and analyzing compound dry and hot events at sub-monthly scale. To achieve this aim, we combine a daily scale drought index, the standardized antecedent precipitation evapotranspiration index (SAPEI), which simultaneously considers precipitation and potential evapotranspiration, with a daily scale standardized temperature index (STI). We investigate the characteristics such as frequency, duration, severity, and intensity of compound dry-hot events during the historical (1961-2018) period and project their changes in China for the future (2050-2100) under different emission scenarios. This index can provide a new tool to quantify the characteristics of compound dry-hot event, and can monitor the compound dry-hot event at multiple time scale (e.g., daily, weekly and monthly) to provide detailed information on their initiation, development, decay, and trends.

2 Methods

2.1 data

Daily meteorological datasets covering 1961 to 2018 were collected from 2239 observational stations across the non-arid region in China (Fig. 1), which include precipitation~~ (P)~~, maximum air temperature~~ (T_{max})~~, mean air temperature~~ (T_{men})~~, minimum air temperature~~ (T_{min})~~, relatively humidity~~ (RH)~~, wind speed~~ (WS)~~, and sunshine duration. All of these meteorological data with strict quality control are available from the China Meteorological Administration (http://cdc.nmic.cn/home.do) and the Resources and Environmental Science Data Center, Chinese Academy of Sciences (http://www.resdc.cn/Default.aspx). ~~The kriging method was applied to interpolate these~~ The observational station data were interpolated to~~into~~ 0.25× 0.25° gridded data by kriging method~~.~~, as ~~-~~it yields higher interpolation accuracy than the other commonly used methods, e.g., ordinary nearest neighbor and inverse distance weighting (Liu et al., 2016). In this study, we only focus the non-arid region in China, because of three reasons: (1) replenishment of water resources across Chinese arid region is mainly from melted glacial or perennial frozen soil, but not from precipitation. The statistical drought indices are usually limited its role in revealing drought in such complex situation; (2) meteorological observations in Chinese arid regions are too scarce to conduct robust analysis (Wu et al., 2007; Xu et al., 2015); (3) from a practical perspective, calculating climate extreme indices across arid region with large-scale desert regions is less meaningless (Tomas-Burguera et al., 2020).

The two commonly used indices (i.e., monthly Palmer d~~D~~rought s~~S~~everity i~~I~~ndex (PDSI) and ~~Standardized~~ standardized p~~P~~recipitation e~~E~~vapotranspiration i~~I~~ndex (SPEI) were employed for comparison. PDSI and SPEI were computed from the same meteorological data described above. The conventional PDSI was empirically derived using the meteorological data of the central USA with its semi-arid climate. The portability of the conventional PDSI is thus relatively poor (Liu et al., 2017). In this study, PDSI was calculated according to the China national standard of classification of meteorological drought with standard number of GB/T 20481-2017. The PDSI ~~calculation procedure of this standard~~ was built based on long-term meteorological data of in-situ stations evenly distributed around China, hence well monitor drought in China (Zhong et al., 2019a), and the detailed calculation on the PDSI is shown in supplementary materials. The 0.25°-daily root zone (0 - 100 cm) soil moisture dataset obtained from Community Land Model ~~(CLM)~~ of the Global Land Data Assimilation System ~~(GLDAS)~~ was also used in this study. Community Land Model product does not have explicit vertical levels, instead soil moisture is represented in surface (0-2cm), and root zone (0-100cm). Root zone soil moisture is chosen over the surface soil moisture on account of its appositeness to characterize drought, low noise relative to surface soil moisture (Hunt et al., 2009; Osman et al., 2020). The dataset from 1961 to 2014 were downloaded from the Goddard Earth Sciences Data and Information Services Center (Rodell et al., 2004). The ~~GLDAS CLM~~ soil moisture dataset from Community Land Model can captures dry and wet conditions in China well (Bi et al., 2016; Feng et al., 2016). To avoid the effect of seasonality, the soil moisture was fitted by Gamma probability distribution, and then was standardized by normal quantile transformation. In addition, 8-day leaf area index ~~(LAI)~~ of the MOD15A2H from 2003 to 2018 were collected. These data were resampled to 0.25° spatial resolution, and then the Z-score was used to calculate the leaf area index~~LAI~~ anomalies.

We further used eight global climate models from the Coupled Model Intercomparison Project Phase 5 (https://esgf.llnl.gov/) (Taylor et al., 2012), including

CanESM2, CNRM-CM5, CSIRO-Mk3.6, MIROC-ESM, MPI-ESM-LR, BCC-CSM1-1, IPSL-CM5A-LR, and MRI-CGCM3, were used to project the future climate conditions. These ~~GCMs~~ global climate models exhibit good performance to simulate the key features of precipitation and temperature in China (Jiang et al., 2016; Yang et al., 2019). We obtained daily climate variables (i.e., precipitation, temperature, relatively humidity, wind speed, ~~P, T_{max}, T_{min}, T_{men}, WS, RH,~~ and shortwave and longwave radiations) for the ~~historical (1961-2005) and~~ future (~~2030~~2050-2100) periods for the three Representative Concentration Pathways (RCPs) including RCP 2.6 (low emission scenario), RCP 4.5 (moderate emission scenario) and RCP 8.5 (high emission scenario). All of the global climate models~~GCM~~ outputs were based on the first ensemble member of each model, referred to as *r1i1p1* in all of the experiments. In this study, the bias-corrected climate imprint method, one of the delta statistical downscaling methods, was used to downscale the global climate models outputs to a spatial resolution of 0.25° (Werner and Cannon, 2016). The detailed information on these global climate models~~GCMs~~ is shown in Table S1.

2.2 Development of SCDHI

The SCDHI is a compound drought and heat index based on a daily drought index and the ~~Standardized Temperature Index (~~STI~~)~~, which is computed in a similar fashion as the Standardized Precipitation Index (Zscheischler et al., 2014). The calculation of daily STI is similar to monthly STI, but for standardizing daily temperature. For example, with respect to one certain grid point, the 1 January STI are computed on the 1 January temperature datasets observed during 1961-2018 at each grid point. We firstly formulated a daily scale drought index, i.e. the ~~standardized antecedent precipitation evapotranspiration index (~~SAPEI~~)~~, by considering both precipitation and potential evapotranspiration~~PET~~. The Penman-Monteith method is used to calculate the potential evapotranspiration, requiring temperature, relatively humidity, wind speed, and sunshine duration. Afterward, the joint distribution method was employed to compute the SCDHI.

2.2.1 Formulation of daily-scale drought index

Li et al. (2020b) have proposed the daily-scale drought index (SAPEI) that considers both precipitation and potential evapotranspiration~~PET~~. However, the primary limitation of this index is that it has a fixed temporal scale and cannot reflect the dry and wet condition at different time scales. Hence, in this study, we developed the multiple time scale (i.e., 3-, 6-, 9-, and 12-month) daily drought index. Here, we followed the same nomenclature proposed by Li et al. (2020b) to refer to a daily standardized drought index (SAPEI) based on precipitation and potential evapotranspiration~~PET~~. SAPEI is simple to calculate, and uses the antecedent accumulative differences between precipitation and potential evapotranspiration~~PET~~ to represent the dry and wet condition of the current day. The calculation procedure is described below.

The Penman-Monteith method (Allen et al., 1998) was firstly used to compute potential evapotranspiration~~PET~~. With a value for potential evapotranspiration~~PET~~, the daily difference between precipitation and potential evapotranspiration~~PET~~ was calculated to reveal climatic water balance (precipitation minus potential evapotranspiration~~PET~~). To reflect dry and wet conditions of the day, the antecedent water surplus or deficit ~~(D)~~ (WSD) was calculated through the following equations:

$$WSD = \sum_{i=1}^{n} (P - PET)_i \qquad (1)$$

Where n ~~n~~ is the number of previous days, PET represents the potential evapotranspiration, and P represents precipitation.

The WSD~~D~~ values can be aggregated at different time scales, such as 3, 6, 9 months, and so on. A probability distribution was used to fit the daily time series WSD~~D~~. Given that different probability distributions may cause differences in drought indices (Stagge et al., 2015), to select the most suitable distribution, several commonly probability distributions including the general extreme value, log-logistic, lognormal, Pearson III, generalized Pareto, exponential, and normal distributions, should be used to fit the WSD~~D~~ series. In the study of Li et al. (2020b), Shapiro-Wilk and Kolmogorov-Smirnov ~~(KS)~~ test have been used applied for optimal probability distribution selection by comparing the empirical probability distribution with a candidate theoretical probability distribution. –They suggested that the log-logistic distribution is more suitable for SAPEI. Moreover, previous researches have demonstrated that the log-logistic distribution is suitable for standardizing drought indices, e.g. SPEI (Vicente-Serrano et al., 2010). Therefore, we chose the log-logistic distribution to compute SAPEI. Once the daily WSD~~D~~ series were fit to a probability distribution, cumulative probabilities of the WSD~~D~~ series were obtained and transformed to standardized units (SAPEI) using the classical approach of Barton et al. (1965).

2.2.2 Construction of SCDHI

The SCDHI was established through copula theory (a brief introduction on copula theory is shown in supplementary materials), which can combine the candidate variables into one numerical expression. This approach not only realizes a projection from multiple dimensions to a single dimension~~a single dimension~~, but also the marginal distributions of the candidate variables combined with their original structures can be fully preserved within the constructed joint distribution. Hence, the copula-based index provides an objective description of the compound events (Hao et al., 2018b; Terzi et al., 2019).

There are many copula families available, which have widely been used for jointing bivariate distributions (Terzi et al., 2019~~; Zhang et al., 2018~~). Among then, Clayton, Gumbel, Normal, T, and Frank copula perform well for jointing bivariate hydrometeorological variables (Ayantobo et al., 2018; Liu et al., 2019), and thus were employed to establish the bivariate joint probability distribution in this study. Assuming, the two random Gaussian variables X and Y representing SAPEI and STI, respectively, the compound dry-hot event~~CDHE~~ can be identified as one variable X lower than or equal to a threshold x, and the other variable Y higher than a threshold y at the same time. The joint probability p of the compound dry-hot event ~~CDHE~~ can then be expressed as:

$$p = P(X \le x, Y \ge y) = u - c(u,v) \qquad (2)$$

where u was the X marginal distribution, and $c(u,v)$ was the joint probability distribution.

This joint cumulative probability p could be treated as an indicator, where smaller p values denote more severe condition of compound dry-hot event~~CDHE~~. However, p to the given marginal sets, p values in different seasons or areas reflected different conditions and are thus not comparable. Hence, the joint probability p was transformed to a uniform distribution by fitting a distribution F, which was then standardized as an indicator to characterize compound dry-hot events ~~CDHEs~~. Once the p series at each day were fitted to a copula, the p series were transformed to standardized units. SCDHI can be estimated by taking the inverse of joint cumulative probability (p) as:

$$SCDHI = \varphi^{-1}(F(P(X \leq x, Y \geq y))) \qquad (3)$$

where φ is the standard normal distribution function. the distribution F was estimated based on the Yeo-Johnson transformation formula (Yeo and Johnson, 2000).

Following the categories of compound dry and hot conditions as suggested by (Wu et al., 2020), we defined five categories of compound dry and hot conditions, including abnormal, light, moderate, heavy and extreme compound drought-hot, as shown in Table 1.

We used Akaike information criterion~~ (AIC)~~, Bayesian information Criterion~~ (BIC)~~, and Kolmogorov-Smirnov~~KS~~ statistics as goodness-of-fit measures to select an appropriate copula. These statistical measures have been commonly used for estimating the goodness of fit of a proposed cumulative distribution function to a given empirical distribution function (Liu et al., 2019; Terzi et al., 2019). The ~~AIC, BIC, and KS~~ statistics of the three metrics are presented in Fig. S1-3. According to the evaluation metrics~~, there was a good agreement between the empirical and parametric copulas. Particularly, the performance of Frank copula slightly outweighed those of the other three copulas. Therefore~~, the Frank copula was utilized to establish the joint probability function and construct SCDHI in this study. Note that the SCDHI under three future scenarios is also used the Frank copula, while the parameters are assessed by future scenarios data. The SCDHI development was illustrated in Fig. S4.

Furthermore, to verify the ability of SCDHI to capture the compound dry and hot event, three verification metrics were used (i.e., probability of detection~~ (POD)~~, false alarm ratio~~ (FAR)~~, and critical success index~~ (CSI)~~) (Winston and Ruthi, 1986~~Zhang et~~

~~al., 2018~~).

$$\cancel{\Pr obability\ of dection = hit/(hit+miss)}$$

$$\textit{Probability of detection} = hit/(hit + miss) \tag{4}$$

$$False\ alarm\ ratio = false\ alarm/(\mathrm{hit} + false\ alarm) \tag{5}$$

$$Critical\ success\ index = hit/(hit + false\ alarm + miss) \tag{6}$$

where *hit* ~~*H*~~ (~~Hit,~~ observed drought-hot) refers to the number of grids when SAPEI and STI is subjected to grade 1-4~~grade 1 (G1) – grade 4 (G4)~~ and SCDHI is subjected to grade 1-4~~G1-G4~~; ~~*M*~~ ~~(~~*Miss*~~)~~ denotes the number of grids when SAPEI and STI is between grade 1-4~~G1 to G4~~ and SCDHI is subjected to other grades than grade 1-4~~G1-G4~~; ~~*F*~~ ~~(*false*~~ *False alarm*~~)~~ denotes the number of grids when SAPEI and STI is subjected to other grades than grade 1-4~~G1-G4~~ but SCDHI is subjected to grades of grade 1-4~~G1-G4~~.

3 Results and Discussion

3.1 Evaluation of SAPEI

The SCDHI was established based on the STI and daily-scale drought index, i.e., SAPEI. However, no previous studies have tested the (daily) drought monitoring performance of SAPEI. When developing a drought index, rigorous testing is required with respect to its applicability before it is applied in drought monitoring. Fig. 2 shows the spatial distributions of the correlations between SAPEI and SPEI/PDSI/soil moisture across China. The monthly mean SAPEI at 3-, 6-, 9- and 12-month scale all showed strong agreement with the SPEI in China, with correlation coefficients higher than 0.8 ($p < 0.01$), indicating that the monthly SAPEI at multiple time scale calculated from the daily value could have the same capability of monthly drought monitoring as

SPEI. The 3-, 6-, 9- and 12-month SAPEI generally showed good correlation with PDSI, and 3-month SAPEI and PDSI generally correlate closely, with correlation coefficients higher than 0.6 ($p < 0.01$)~~, while the 12-month SAPEI displayed weak correlation with PDSI in south China~~. For daily SAPEI at ~~3~~12-month scale and soil moisture, a close correlation was detected in south and north China, while relatively weak correlation is found in ~~north~~ Midwest China. The correlation between SAPEI and soil moisture increased in magnitude ~~and spatial extent~~ at time scales of ~~6~~3-~~12~~ 9 months. For 12-month SAPEI, mean correlation coefficient ~~was~~ reached 0.5~~generally greater than 0.6~~ for ~~a majority of~~ whole China. This phenomenon implied that the short-time scale SAPEI was more sensitive to precipitation change, and thus could be more suitable for meteorological drought, while the long-time scale (more than five month) SAPEI was more closely related to soil moisture and can be applied for agricultural drought monitoring. Overall, these analyses indicate that the SAPEI at daily and monthly scale showed reliability in drought monitoring.

To further test the drought monitoring performance of the SAPEI, typical drought events were chosen as case studies. During recent decades, several well-known large-scale drought events have hit China, including the droughts in winter of 2009 to spring of 2010, and in 2011 (Lu et al., 2014; Yu et al., 2019). In this study, the drought regimes during these events were taken as case studies to evaluate the drought monitoring performance of SAPEI at 3-~~ and 6-~~month time scales (Sun and Yang, 2012). We firstly showed the monthly evolution of these events by the monthly mean SAPEI, SPEI, and PDSI, and then analyzed the daily evolution of drought in space and time in the most affected areas according to SAPEI and soil moisture.

3.2.1 Drought events during 2009-2010

~~Fig. S5 illustrates the monthly changes in the 2009/10 drought monitored by the~~

~~PDSI, SPEI, and SAPEI at 3- and 6-month scale.~~ As shown in Fig. S5, the monthly evolution in 2009/10 drought based on SAPEI was generally similar with that of SPEI and PDSI. This drought started to appear in most of China (except for the central and northeast China) in September 2009, and then persisted in most of China during October to December 2009.~~; during this period, drought conditions became more severe in south China.~~ During January and April in 2010, severe drought persisted in southwest China~~The drought in north and east China gradually faded away during January and March in 2010. In contrast, in southwest China (SWC) the drought intensity became rather strong during the same period. The severe dry condition continued in SWC during April in 2010~~, while drought in the rest of China gradually disappeared in this period. After that, dry conditions in southwest China~~SWC~~ gradually relieved from May to June in 2010, but did not disappear. ~~The monthly drought evolution based on SAPEI was generally similar with that of SPEI and PDSI.~~

Despite being located in the humid climate zone, southwest China~~SWC~~ suffered from exceptional drought during the autumn of 2009 to the spring of 2010 (Lin et al., 2015). During this drought, more than 16 million people and 11 million livestock faced drinking water shortages, with direct economic losses estimated at 19 billion yuan in southwest China~~SWC~~ (Lin et al., 2015). We selected this event in southwest China~~SWC~~ as the first case study, and reveal detailed spatial and temporal change of this event at daily scale based on SAPEI and soil moisture (Fig. 3 and 4). During September 1 to 30 of 2009, the drought started to appear in the region, and dry conditions became worse and spread throughout nearly the entire southwest China~~SWC~~ from October 1 to November 15 of 2009. Severe dry conditions then stayed in the region for 152 days from November 15 to April 15 of 2010, with high intensity. Afterwards, severe drought was gradually relieved from April 15 to June 15. The drought diminished over time in most parts of southwest China by the end of June.

3.2.2 Drought events in 2011

~~The monthly changes in the 2011 drought is illustrated in~~ As shown in Fig. S6. The 2011 drought monthly pattern monitored by SAPEI are generally consistent~~shows a good agreement~~ with those by SPEI and PDSI. ~~More specifically, t~~The drought mainly started in north China in January, while in March it spread to most of China, and severe dry conditions persisted in most areas during April to May.~~, and drought conditions in lower reaches of the Yangtze River basin became serious. In April to May, severe dry conditions persisted in the middle and lower reaches of the Yangtze River Basin (MLR-YRB), and extended from the YRB to southern China.~~ In August, the drought mainly moved to southward~~westward and reached the edge of southwestern China~~. Severe drought persisted in ~~the region~~southwest China during September and October, but it then gradually faded away~~ in November and December~~. The results monitored by the SAPEI are generally consisted with the findings of Lu et al. (2014).

The 2011 drought event was particularly unusual in the middle and lower reaches of the Yangtze River Basin (MLR-YRB). The MLR-YRB is generally in a wet condition, nevertheless, suffered its worst drought in the 50 years during the spring. The severe drought caused shortage of drinking water for 4.2 million people. 3.7 million hectares of crops were damaged or destroyed. Moreover, the heavy drought led to more than 1,300 lakes devoid of all water in Hubei province (Xu et al., 2015). The temporal and spatial evolution of this event in MLR-YRB described by daily SAPEI and soil moisture was shown in Fig. 5-6. The drought started to appear in the north part of the MLR-YRB in early February of 2011, and then gradually expanded to the whole MLR-YRB during early February and March 15. The severe drought condition persisted in this region for 78 days (from March 15 to May 31). Afterwards, there was a tendency toward alleviating drought conditions, and most of MLR-YRB was under light and moderate drought conditions.

The previous detailed analysis showed that the SAPEI not only captures monthly characteristics of droughts, but also has the potential to track droughts at sub-monthly scale (Li et al., 2020b). Though the input data (including precipitation and potential evapotranspiration~~PET~~) of SAPEI are similar to SPEI, the rationale of the index is different from SPEI. It was calculated for each day and considers the water surplus or deficit of that day and the previous days. SPEI was commonly employed to monitor and analyze the monthly or longer-scale droughts (Vicente-Serrano et al., 2010). It thus may not be appropriate to apply the SPEI at shorter timescales (e.g., daily or weekly), because of the inherent problem in the construction of the index. Although SPEI gives a full and equal consideration to the water surplus or deficit in the period of the considered time scale, it does not consider the water surplus or deficit in the days before the period. If the scale is very short, this may cause problems. For a 7-day period, for example, if there is no precipitation during the period, it may be regarded as a drought period when compared with historical records (the method used by the SPEI); however, if there is a heavy precipitation just before the period, then the 7-day period probably remains wet and is unlikely to experience drought condition during such a short time. Previous studies have demonstrated the disadvantage of SPEI for short-time scale drought monitoring (Lu, 2009; Lu et al., 2014; Li et al., 2020b).

Soil moisture would be the most appropriate variable for agriculture drought monitoring and analyses (Mishra and Singh, 2010). However, there are few long-term and large-scale observational soil moisture datasets due to insufficient observation stations around the world, especially for developing regions, which limits it wide use in drought monitoring and analyses (Seneviratne et al., 2010). Thus, using observational hydrometeorological datasets, the complex physical process models, such as the variable infiltration capacity model, are widely used to simulate the soil moisture (Liang et al., 1996; Xia et al., 2018). However, running such models requires highly trained personnel not usually available at local agencies. In addition, when the model is used locally, it generally needs to be calibrated and verified by observational soil moisture and other hydrometeorological datasets (Xia et al., 2018; Zhou et al., 2019). This certainly limits the wide use of soil moisture as a drought indicator.

In summary, the SAPEI meets the requirements of a drought index, given the fact that it shows reliable and robust ability for drought analysis and monitoring. Like the SPEI, SAPEI includes multiple time scales (3-, 6-, 9-, and 12- month) to monitor droughts at monthly resolution and is relatively sensitive to soil moisture variation. However, SAPEI has the advantage over SPEI regarding sub-monthly drought monitoring. Such an index could help fill a gap between science and applications in that it would be operationally tractable for detecting and monitoring both short-term and sustained droughts.

3.2 Evaluation of SCDHI

The SCDHI was developed by joining~~joining~~ the marginal distribution of the SAPEI and STI. Though the copula method has been widely utilized to connect bivariate distribution, the property of SCDHI in capturing compound dry-hot events~~CDHEs~~ still needs to be tested. ~~Fig. 7 shows the spatial distributions of the correlations between SCDHI and SAPEI/STI at daily scale across China. The SCDHI all showed strong (p < 0.01) correlation with the SAPEI at 3-, 6-, 9- and 12-month scale in China, with correlation coefficients higher than 0.7. A significant correlation (p < 0.01) was also detected between STI and SCDHI at multiple scales.~~ Fig. ~~8~~ 7 shows the spatial pattern ~~in~~ and density plot for probability of detection~~POD~~, false alarm ratio~~FAR~~, and critical success index~~CSI~~ when the drought and hot events observed by SAPEI and STI, respectively, were related to compound drought-hot event detected by SCDHI at 3-, 6-, 9- and 12-monthly scale. As shown in Fig. ~~8~~7, probability of detection~~POD~~ is close to 1 and false alarm ratio~~FAR~~ is close to 0, implying that SCDHI can well detect in most of the areas where the droughts and hots were detected by SAPEI and STI. The values of critical success index~~CSI~~ indicated that the ratios of drought-hot affected areas detected by SAPEI and STI to the drought and hot areas detected by SCDHI were close to one. Overall, these analyses implied that SCDHI can well monitor droughts and hots that can be successfully captured by SAPEI and STI. The SCDHI thus detects compound dry-hot events~~CDHEs~~ that are identified separately by the coincidence of low SAPEI and high STI. In addition, the SCDHI detects events that are very extreme in either the SAPEI or the STI and moderate in the other variable but thus still cause substantial damage (Zscheischler et al., 2017b). Furthermore, the SCDHI is able to quantify the magnitude of compound dry-hot events~~CDHEs~~.

To further test the drought-heat monitoring performance of the SCDHI, two typical ~~CDHE~~compound dry-hot events were chosen as case studies according to the Yearbook of Meteorological Disasters in China. One was a well-known compound drought and heatwave striking Sichuan-Chongqing region~~ (SCR)~~ with serious consequences during summer of 2006 (Wu et al., 2020), and the other occurred in southern China with adverse impacts on agriculture during July to September of 2009 (Wang et al., 2010). Sichuan-Chongqing region~~SCR~~ experienced continuous extreme temperature during mid-June to late August 2006. The duration and severity of this hot event were the worst on the historical record. Simultaneously, a heavy drought occurring once in 100 years hit this region. During this compound event, a population of over ten million was confronted with drinking water shortage, about twenty thousand km^2 of cropland suffered serious losses, and more than one hundred times forest fire broke out. Local governments issued the most serious arid warning (Zhang et al., 2008). Thus, we take this typical drought-hot event as first case studies to evaluate the drought/hot monitoring performance of SCDHI. The monthly spatial pattern of this compound event in Sichuan-Chongqing region~~SCR~~ is shown in Fig. S7, indicating that Sichuan-Chongqing region~~SCR~~ during summer in 2006 experienced the moderate to extreme compound dry and hot conditions. Fig. ~~9~~ 8 maps the spatial pattern of this compound event and its impact on vegetation from mid-June to late August. This event started to appear in Sichuan-Chongqing region~~SCR~~ in mid-June 2006, and gradually spread throughout the whole Sichuan-Chongqing region~~SCR~~ during June 19 to 26. The moderate dry-hot condition then persisted in the entire Sichuan-Chongqing region~~SCR~~ from June 27 to August 5 in 2006, lasting for 40 days. The negative leaf area index~~LAI~~ was scattered in some of the dry-hot affected areas. However, during August 6 to 21, the drought-hot event became even more severe with the onset of extremely hot temperatures, causing negative vegetation anomalies in most of the affected areas.

The monthly spatial pattern of another compound event in southern China during July to September of 2009 is shown in Fig. S8. Overall moderate to heavy compound dry and hot conditions are observed at monthly scale in this region. However, this event showed large fluctuation at weekly scale. According to the Yearbook, the hot event was divided into two periods: the first stage was from early to late July, and the other stage was from mid-August to early September. The fluctuating compound event caused adverse impact of crop pollination and grain filling, resulting in decrease of crop production. Fig. ~~10~~ 9 maps the spatial pattern of this event and its impact on leaf area index~~LAI~~. In the first stage, the drought-hot event hit the most of southern China during July 5 to 12, and then it became severe in the west part of southern China during July

13 to 20. However, the hot event suddenly disappeared from July 21 to 28, leading to disappearance of the compound event in most of southern China (Fig. 9~~10~~a). Afterward, the compound event hit this region again from August 6 to 13, and its intensity was strong during August 14 to 21, with severe hot conditions. Subsequently, the intensity and spatial extent of the compound event faded away in north of southern China during August 22 to 29. This event extended to most of this region again from August 30 to September 14, with severe dry and hot condition. The compound events still stayed in this region from September 15 to 22 (Fig. ~~10b~~9b). Despite the short-term event, the anormal change in vegetation was found in most of the dry-hot affected areas. This complex event~~event~~ indicates that monthly analyses of the event can provide an overall situation, but is not be able to~~is~~ ~~not be able to~~ capture the serious dry and hot conditions caused by a short-term extreme climate anomaly at shorter time scales. Though such short-term compound event only lasted for days or weeks, they lead to large agricultural losses if they occur within sensitive stages in crop development (i.e., pollination and grain filling) (Mazdiyasni and AghaKouchak, 2015). To provide timely information of the compound dry-hot events~~CDHEs~~, short-time scale analyses and monitoring of such events are essential.

Overall, the changes in these two compound dry-hot events~~CDHEs~~ based on SCDHI are consistent with the national weather records~~reports~~ (http://www.weather.com.cn/zt/kpzt/) and the Yearbook of Meteorological Disasters in China 2010~~(http://www.weather.com.cn/)~~. In summary, the SCDHI is able to robustly and reliably capture compound dry-hot events~~CDHEs~~ at sub-monthly scale, and potentially provide a new tool to objectively and quantitatively analyze and monitor the characteristics of compound dry-hot events~~CDHEs~~ in time and space.

3.3 Application

Here, we evaluate and compare the spatiotemporal variation of characteristics of compound dry-hot events~~CDHEs~~ in China during growing season (April-September), because such events can easily cause adverse impact on agriculture and ecosystem during these periods (Hao et al., 2018; Wu et al., 2019). More precisely, the compound dry-hot events~~CDHEs~~ ~~during growing season (April-September)~~ from 1961 to 2018 were identified based on 3-month scale SCDHI and run theory (Wu et al., 2018), after which the frequency, duration, severity, and intensity of these events were analyzed (A specific case to identify compound dry-hot event~~CDHE~~ is shown in Fig. S9). We then projected their future characteristics changes under the RCP 2.6, 4.5 and 8.5 from 2050 to 2100. Given that short-term concurrent dry and hot events generally persist for at least weeks (Otkin et al., 2018), only the events lasting for more than two weeks were considered in this study.

Fig. ~~11~~ 10 shows spatial patterns of characteristics of the compound dry-hot events ~~CDHEs~~. A high frequency of compound events was detected in southern China, with occurrence of every two years on average, in contrast, the eastern Tibet Plateau and northeast China experienced fewer compound events (Fig. ~~11a~~10a), which was generally consistent with the previous studies (Liu et al., 2020; Wang et al., 2016). The compound dry-hot event~~CDHE~~ generally lasted for about twenty-five to thirty-five days in most of China, while in east Tibet Plateau, the compound dry-hot event~~CDHE~~ persisted for less than twenty days (Fig. ~~11b~~10b). The severity and intensity of the compound dry-hot event~~CDHE~~ presented relatively similar patterns and showed that most of eastern China experienced high severity and intensity (Fig. ~~11~~ 10c-d). Overall, southern China suffered more frequent compound dry-hot events~~CDHEs~~, with higher severity and intensity. Southern China is a humid region where evapotranspiration is mainly controlled by energy supply because soil moisture is usually sufficient. For given adequate soil moisture in the initiation of drought, evaporative demand can increase rapidly during a short period when strong, transient meteorological changes (such as extreme temperature) occur, which in turn exhaust soil moisture to intensify drought conditions (Zhang et al., 2019, Otkin et al., 2018). Moreover, vegetation over south China is usually abundant and plants tend to suck more water from the soil when high temperatures occur, causing evapotranspiration increase and soil moisture decline (Li et al., 2020c; Wang et al., 2016). More surface sensible heat fluxes are thus transferred to the near-surface atmosphere to further increase air temperatures (Mo and Lettenmaier, 2015). These land-atmosphere interactions altogether cause the Bowen ratio to increase (Otkin et al., 2013, 2018), creating a favorable condition for short-term concurrence droughts and hots. Therefore, compound dry-hot event are more likely to occur in humid regions with higher severity and intensity.

Fig. ~~12~~ 11 illustrates the spatial patterns of change in frequency, duration, severity, and intensity of the compound dry-hot events~~CDHEs~~ under RCP 2.6, 4.5, and 8.5 scenarios. According to Fig. ~~12a~~11a, the future (2050-2100) compound dry-hot event~~CDHE~~ frequency under three scenarios in most of east China will increase by about one to three times with respect to the reference period (1961-2018). Under RCP 8.5 scenario, compound dry-hot event~~CDHE~~ at about 4% of the study region is expected to markedly increase by more than five times, which are scattered in the central to west parts of China. The duration of compound dry-hot event~~CDHE~~ across the east of the study region will mainly show an increase of about 0.5 times, while duration in mid-west China potentially increases by approximately 1.5 times under RCP 8.5 scenarios (Fig. ~~12b~~11b). The spatial pattern of future severity change is similar to the duration; severity in most of east China is projected to increase by about 0.5 time under three scenarios; however, compound dry-hot event~~CDHE~~ severity over mid-west China is expected to more than triple under RCP 8.5 (Fig. ~~12c~~11c). The compound dry-hot event~~CDHE~~ intensity in most of the study region exhibits slight increase for all scenarios in comparison to the historical period.

~~The cumulative density functions (CDFs) of the CHDE frequency, duration, severity, and intensity in historical and future periods were quantified, and the result is shown in Fig. 13. A substantial change in the values of CHDE frequency, duration, severity, and intensity was detected between the historical and future projections. The frequency, duration, severity, and intensity of CHDEs will intensify throughout the China in future scenarios compared to the historical reference, as marked by the movement towards the right side of the CDF curves. Specifically, the cumulative probability of CDHE frequency is expected to increase by more than 80% under three scenarios, compared with the 95~~th ~~percentile value in historical period (Fig. 13a). The cumulative probability of duration would increase by about 72% under RCP 8.5 scenario, while increment under RCP 2.6 scenario is relatively small (17%), in comparison to the 95~~th ~~percentile in reference period (Fig. 13b). The severity cumulative probability project to increase by 42% and 53% under RCP 2.6 and 4.5 scenarios respectively, but even increase by 88% under RCP 8.5 scenario (Fig. 13c). An increase of at least 42% is observed in the intensity cumulative probability, compared with the n reference period (Fig. 13d). Such an increase in the frequency, duration, severity, and intensity of CDHEs across China could be a new normal in future.~~

Global warming is very likely to exacerbate the prevalence of the compound dry-hot events~~CDHEs~~ (Pfleiderer et al., 2019). ~~Trends are often present in individual variables (e.g., temperature, and precipitation), while can also occur in the dependence between drivers of compound events, which consequently affects associated risks. The~~

~~(negative) correlation between seasonal mean summer temperature and precipitation is projected to intensify in many land regions, leading to more frequent extremely dry and hot conditions (Kirono et al., 2017; Zscheischler and Seneviratne, 2017a).~~ The cumulative density functions of the future variations in compound dry-hot event characteristics considering only temperature and all variable changes were quantified, and the result is shown in Fig. 12. The frequency and intensity of the future variations in compound dry-hot event do not show large difference between two scenarios (i.e., temperature and all variable changes), while duration and severity display great increase due to temperature variation, as marked by the movement towards the right side of the cumulative density curves. Increasing temperature could lead to remarkable increase evapotranspiration, and thus causing more surface sensible heat fluxes into atmosphere (Mo and Lettenmaier, 2015; Zhang et al., 2019). These land-atmosphere interactions altogether cause the Bowen ratio to increase (Otkin et al., 2013, 2018), creating a favorable condition for concurrence dries and hots. In short, temperature could be generally the primary factor increasing the compound dry-hot severity and duration (Cook et al., 2014). In addition, trends are often present in individual variables, while can also occur in the dependence between drivers of compound events, which consequently affects associated risks. The (negative) correlation between seasonal mean summer temperature and precipitation is projected to intensify in many land regions, leading to more frequent extremely dry and hot conditions (Kirono et al., 2017; Zscheischler and Seneviratne, 2017a), while variation in compound dry-hot event due to the complex interaction between climate variables is need further studied (Zscheischler et al., 2020). Overall, the frequency, severity, duration, and intensity of the compound dry-hot events~~CDHEs~~ in China under global warming will increase significantly. Effective measures need to be implemented to decrease the CO^{2}emissions for compound dry and hot event mitigation.

4 Conclusions

Under global warming, the compound dry and hot event tends to more frequent and short-lived (i.e., days or weeks). Correspondingly, a compound drought and heat index should be able to monitor such event at sub-monthly scales in order to timely reflect dry and hot condition evolution. In this study, we developed a multiple time scale (e.g., 3-, 6-, 9, and 12- month) compound drought and heat index, termed as SCDHI, to monitor short-time (e.g., days or weeks) and long-time (e.g., months) compound event. This index was established based on the daily drought index (i.e., SAPEI) and Standardized Temperature Index (STI) using a joint probability distribution method. Using the SCDHI, we then quantitatively investigated the characteristics (i.e., frequency, intensity, severity, and duration) of the compound dry-hot event~~CDHE~~s in China in historical period (1961-2018), and revealed how they would change in the future (2050-2100) under representative concentration pathway (RCP) 2.6, 4.5, and 8.5 scenarios. The main conclusions of this study are presented as follows: The SCDHI can well monitor simultaneous dries and hots detected by SAPEI and STI. The monthly SCDHI can provide an overall situation of the compound dry and hot conditions, but sub-monthly SCDHI can well capture fluctuation of simultaneous dries and hots within a month. It also can reflect the impact of the compound dry and hot event on vegetation anomalies. The SCDHI can offer a new tool to quantitatively measure the characteristics of the compound dry-hot event~~CDHE~~s. It also can provide detailed information such as the initiation, development, decay, and tendency of the compound event for decision-makers and stakeholders to make early and timely warning. In the case study of the China, the southern China suffered more frequent the compound dry-hot event~~CDHE~~, with higher severity and intensity. The compound dry-hot event~~CDHE~~

mainly lasted for twenty-five to thirty-five days in China. The frequency, duration, severity, and intensity of compound events will intensify throughout the China in future. The frequency will increase by about one to three times with respect to the reference period. A region with fewer compound event (< 5) would exhibit a multi-fold (more than five times) increase in the future. The duration across east areas mainly increased by 0.5 times, while severity project to increase by about 0.5 to 1 times.

Data availability. The observed meteorological datasets are available at http://cdc.nmic.cn/home.do. The CMIP5 datasets are available at https://esgf.llnl.gov.

Author Contributions. Conceived and designed the experiments: JL, ~~WS~~SW. Performed the experiments: JL, ~~WS~~SW. Analyzed the data: JL. Wrote and edited the paper: JL, ~~WS~~SW, ~~WZ~~ZW, ~~ZJ~~JZ, ~~GS~~SG, ~~CX~~XC.

Competing interests. The authors declare that they have no conflict of interest.

Acknowledgement

The research is financially supported by the National Natural Science Foundation of China (51879107, 51709117), the Guangdong Basic and Applied Basic Research Foundation (2019A1515111144), and the Water Resource Science and Technology Innovation Program of Guangdong Province (2020-29).

References

Allen, R. G., Pereira, L. S., Raes, D. and Smith, M.: Crop evapotranspiration: Guidelines for computing crop requirements, Irrig. Drain. Pap. No. 56, FAO, doi:10.1016/j.eja.2010.12.001, 1998.

~~Anderson, M. C., Zolin, C. A., Sentelhas, P. C., Hain, C. R., Semmens, K., Tugrul Yilmaz, M., Gao, F., Otkin, J. A. and Tetrault, R.: The Evaporative Stress Index as an indicator of agricultural drought in Brazil: An assessment based on crop yield impacts, Remote Sens. Environ., doi:10.1016/j.rse.2015.11.034, 2016.~~

Ayantobo, O. O., Li, Y., Song, S., Javed, T. and Yao, N.: Probabilistic modelling of drought events in China via 2-dimensional joint copula, J. Hydrol., 559, 373–391, doi:10.1016/j.jhydrol.2018.02.022, 2018.

Barton, D. E., Abramovitz, M. and Stegun, I. A.: Handbook of Mathematical Functions with Formulas, Graphs and Mathematical Tables., J. R. Stat. Soc. Ser. A, doi:10.2307/2343473, 1965.

Bi, H., Ma, J., Zheng, W. and Zeng, J.: Comparison of soil moisture in GLDAS model simulations and in situ observations over the Tibetan Plateau, J. Geophys. Res., doi:10.1002/2015JD024131, 2016.

Chen, L., Chen, X., Cheng, L., Zhou, P. and Liu, Z.: Compound hot droughts over China: Identification, risk patterns and variations, Atmos. Res., 227(May), 210–219, doi:10.1016/j.atmosres.2019.05.009, 2019.

Cook, B. I., Smerdon, J. E., Seager, R., and Coats, S.: Global warming and 21 st century drying. Climate Dynamics, 43(9-10), 2607-2627, 2014.

Feng, X., Fu, B., Piao, S., Wang, S., Ciais, P., Zeng, Z., Lü, Y., Zeng, Y., Li, Y., Jiang, X. and Wu, B.: Revegetation in China's Loess Plateau is approaching sustainable water resource limits, Nat. Clim. Chang., doi:10.1038/nclimate3092, 2016.

~~Ford, T. W. and Labosier, C. F.: Meteorological conditions associated with the onset of flash drought in the Eastern United States, Agric. For. Meteorol., doi:10.1016/j.agrformet.2017.08.031, 2017.~~

Ford, T. W., McRoberts, D. B., Quiring, S. M. and Hall, R. E.: On the utility of in situ soil moisture observations for flash drought early warning in Oklahoma, USA, Geophys. Res. Lett., doi:10.1002/2015GL066600, 2015.

~~Gallant, A. J. E., Karoly, D. J. and Gleason, K. L.: Consistent trends in a modified climate extremes index in the United States, Europe, and Australia, J. Clim., 27(4), 1379–1394, doi:10.1175/JCLI-D-12-00783.1, 2014.~~

Hao, Z., Hao, F., Singh, V. P., Xia, Y., Shi, C. and Zhang, X.: A multivariate approach for statistical assessments of compound extremes, J. Hydrol., 565, 87–94, doi:10.1016/j.jhydrol.2018.08.025, 2018a.

Hao, Z., Hao, F., Singh, V. P. and Zhang, X.: Quantifying the relationship between compound dry and hot events and El Niño–southern Oscillation (ENSO) at the global scale, J. Hydrol., 567, 332–338, doi:10.1016/j.jhydrol.2018.10.022, 2018b.

Hao, Z., Hao, F., Singh, V. P. and Zhang, X.: Statistical prediction of the severity of compound dry-hot events based on El Niño-Southern Oscillation, J. Hydrol., 572, 243–250, doi:10.1016/j.jhydrol.2019.03.001, 2019.

Hunt, E. D., Hubbard, K. G., Wilhite, D. A., Arkebauer, T. J. and Dutcher, A. L.: The development and evaluation of a soil moisture index. Int. J. Climatol., 29(5), 747-759, doi.org/10.1002/joc.1749, 2009.

James, S., Complex, B., Black, S. J., Health, O. and Ando, H.: The synergy between drought and extremely hot summers in the Mediterranean, Biochem. J., 2010.

Jiang, D., Tian, Z. and Lang, X.: Reliability of climate models for China through the IPCC Third to Fifth Assessment Reports, Int. J. Climatol., doi:10.1002/joc.4406, 2016.

Kirono, D. G. C., Hennessy, K. J. and Grose, M. R.: Increasing risk of months with low rainfall and high temperature in southeast Australia for the past 150 years, Clim.

Risk Manag., doi:10.1016/j.crm.2017.04.001, 2017.

Koster, R. D., Schubert, S. D., Wang, H., Mahanama, S. P. and Deangelis, A. M.: Flash drought as captured by reanalysis data: Disentangling the contributions of precipitation deficit and excess evapotranspiration, J. Hydrometeorol., doi:10.1175/JHM-D-18-0242.1, 2019.

Liang, X., Wood, E. F., and Lettenmaier, D. P.: Surface soil moisture parameterization of the VIC-2L model: Evaluation and modification. Global and Planetary Change, 13(1-4), 195-206, 1996.

Li, J., Wang, Z., Wu, X., Chen, J., Guo, S., and Zhang, Z.: A new framework for tracking flash drought events in space and time. Catena, 194, 104763, 2020a.

Li, J., Wang, Z., Wu, X., Xu, C.-Y., Guo, S. and Chen, X.: Toward Monitoring Short-Term Droughts Using a Novel Daily-Scale, Standardized Antecedent Precipitation Evapotranspiration Index, J. Hydrometeorol., 891–908, doi:10.1175/jhm-d-19-0298.1, 2020b.

Li, J., Wang, Z., Wu, X., Guo, S., and Chen, X.: Flash droughts in the Pearl River Basin, China: Observed characteristics and future changes. Sci. Total Environ., 707, 136074, 2020c.

Lin, W., Wen, C., Wen, Z. and Gang, H.: Drought in Southwest China: A Review, Atmos. Ocean. Sci. Lett., 8(6), 339–344, doi:10.3878/AOSL20150043, 2015.

Liu, Z., Wang, Y., Shao, M., Jia, X., Li, X: Spatiotemporal analysis of multiscalar drought characteristics across the Loess Plateau of China. J. Hydrol., 534, 281-299, doi.org/10.1016/j.jhydrol.2016.01.003, 2016,

Liu, Y., Zhu, Y., Ren, L., Singh, V. P., Yang, X. and Yuan, F.: A multiscalar Palmer drought severity index, Geophys. Res. Lett., 44(13), 6850–6858, doi:10.1002/2017GL073871, 2017.

Liu, Y., Zhu, Y., Ren, L., Yong, B., Singh, V. P., Yuan, F., Jiang, S. and Yang, X.: On the mechanisms of two composite methods for construction of multivariate drought indices, Sci. Total Environ., 647, 981–991, doi:10.1016/j.scitotenv.2018.07.273, 2019.

Liu, Y., Zhu, Y., Zhang, L., Ren, L., Yuan, F., Yang, X. and Jiang, S.: Flash droughts characterization over China: From a perspective of the rapid intensification rate, Sci. Total Environ., doi:10.1016/j.scitotenv.2019.135373, 2020.

Lu, E.: Determining the start, duration, and strength of flood and drought with daily precipitation: Rationale, Geophys. Res. Lett., 36(12), 1–5, doi:10.1029/2009GL038817, 2009.

Lu, E., Cai, W., Jiang, Z., Zhang, Q., Zhang, C., Higgins, R. W. and Halpert, M. S.: The day-to-day monitoring of the 2011 severe drought in China, Clim. Dyn., 43(1–2), 1–9, doi:10.1007/s00382-013-1987-2, 2014.

Mo, K. C. and Lettenmaier, D. P.: Heat wave flash droughts in decline, Geophys. Res. Lett., doi:10.1002/2015GL064018, 2015.

Mo, K. C. and Lettenmaier, D. P.: Precipitation deficit flash droughts over the United States, J. Hydrometeorol., doi:10.1175/JHM-D-15-0158.1, 2016.

Mazdiyasni, O. and AghaKouchak, A.: Substantial increase in concurrent droughts and heatwaves in the United States, Proc. Natl. Acad. Sci. U. S. A., 112(37), 11484–11489, doi:10.1073/pnas.1422945112, 2015.

~~Miralles, D. G., Gentine, P., Seneviratne, S. I. and Teuling, A. J.: Land–atmospheric feedbacks during droughts and heatwaves: state of the science and current challenges, Ann. N. Y. Acad. Sci., 1436(1), 19–35, doi:10.1111/nyas.13912, 2019.~~

Manning, C., Widmann, M., Bevacqua, E., Van Loon, A. F., Maraun, D. and Vrac, M: Increased probability of compound long-duration dry and hot events in Europe during summer (1950-2013). Environmental Research Letters, 14(9), 094006, 2019.

Osman, M., Zaitchik, B. F., Badr, H. S., Christian, J. I., Tadesse, T., Otkin, J. A. and Anderson, M. C.: Flash drought onset over the Contiguous United States: Sensitivity of inventories and trends to quantitative definitions, Hydrol. Earth Syst. Sci. Discuss., doi.org/10.5194/hess-2020-385, in review, 2020.

Otkin, J. A., Anderson, M. C., Hain, C., Mladenova, I. E., Basara, J. B. and Svoboda, M.: Examining rapid onset drought development using the thermal infrared-based evaporative stress index, J. Hydrometeorol., doi:10.1175/JHM-D-12-0144.1, 2013.

Otkin, J. A., Svoboda, M., Hunt, E. D., Ford, T. W., Anderson, M. C., Hain, C. and Basara, J. B.: Flash droughts: A review and assessment of the challenges imposed by rapid-onset droughts in the United States, Bull. Am. Meteorol. Soc., 99(5), 911–919, doi:10.1175/BAMS-D-17-0149.1, 2018.

~~Otkin, J. A., Zhong, Y., Hunt, E. D., Basara, J., Svoboda, M., Anderson, M. C. and Hain, C.: Assessing the evolution of soil moisture and vegetation conditions during a flash drought-flash recovery sequence over the South-Central United States, J. Hydrometeorol., doi:10.1175/JHM-D-18-0171.1, 2019.~~

Pfleiderer, P., Schleussner, C. F., Kornhuber, K. and Coumou, D.: Summer weather becomes more persistent in a 2 °C world, Nat. Clim. Chang., 9(9), 666–671, doi:10.1038/s41558-019-0555-0, 2019.

Rodell, M., Houser, P. R., Jambor, U., Gottschalck, J., Mitchell, K., Meng, C. J., Arsenault, K., Cosgrove, B., Radakovich, J., Bosilovich, M., Entin, J. K., Walker, J. P., Lohmann, D. and Toll, D.: The Global Land Data Assimilation System, Bull. Am. Meteorol. Soc., doi:10.1175/BAMS-85-3-381, 2004.

Röthlisberger, M. and Martius, O.: Quantifying the Local Effect of Northern

Hemisphere Atmospheric Blocks on the Persistence of Summer Hot and Dry Spells, Geophys. Res. Lett., doi:10.1029/2019GL083745, 2019.

Schumacher, D. L., Keune, J., van Heerwaarden, C. C., Vilà-Guerau de Arellano, J., Teuling, A. J. and Miralles, D. G.: Amplification of mega-heatwaves through heat torrents fuelled by upwind drought, Nat. Geosci., 12(9), 712–717, doi:10.1038/s41561-019-0431-6, 2019.

Sedlmeier, K., Feldmann, H. and Schädler, G.: Compound summer temperature and precipitation extremes over central Europe, Theor. Appl. Climatol., doi:10.1007/s00704-017-2061-5, 2018.

Stagge, J. H., Tallaksen, L. M., Gudmundsson, L., Van Loon, A. F. and Stahl, K.: Candidate Distributions for Climatological Drought Indices (SPI and SPEI), Int. J. Climatol., doi:10.1002/joc.4267, 2015.

Seneviratne, S. I., Corti, T., Davin, E. L., Hirschi, M., Jaeger, E. B., Lehner, I., .and Teuling, A. J.: Investigating soil moisture–climate interactions in a changing climate: A review. Earth-Science Reviews, 99(3-4), 125-161, 2010.

Sun, C. and Yang, S.: Persistent severe drought in southern China during winter-spring 2011: Large-scale circulation patterns and possible impacting factors, J. Geophys. Res. Atmos., doi:10.1029/2012JD017500, 2012.

Sun, C. X., Huang, G. H., Fan, Y., Zhou, X., Lu, C. and Wang, X. Q.: Drought Occurring With Hot Extremes: Changes Under Future Climate Change on Loess Plateau, China, Earth’s Futur., 7(6), 587–604, doi:10.1029/2018EF001103, 2019.

Swain, D. L., Langenbrunner, B., Neelin, J. D. and Hall, A.: Increasing precipitation volatility in twenty-first-century California, Nat. Clim. Chang., 8(5), 427–433, doi:10.1038/s41558-018-0140-y, 2018.

Taylor, K. E., Stouffer, R. J. and Meehl, G. A.: An overview of CMIP5 and the experiment design, Bull. Am. Meteorol. Soc., doi:10.1175/BAMS-D-11-00094.1, 2012.

Terzi, S., Torresan, S., Schneiderbauer, S., Critto, A., Zebisch, M. and Marcomini, A.: Multi-risk assessment in mountain regions: A review of modelling approaches for climate change adaptation, J. Environ. Manage., 232(September 2018), 759–771, doi:10.1016/j.jenvman.2018.11.100, 2019.

Vicente-Serrano, S. M., Beguería, S. and López-Moreno, J. I.: A multiscalar drought index sensitive to global warming: The standardized precipitation evapotranspiration index, J. Clim., 23(7), 1696–1718, doi:10.1175/2009JCLI2909.1, 2010.

Wang, L., Yuan, X., Xie, Z., Wu, P. and Li, Y.: Increasing flash droughts over China during the recent global warming hiatus, Sci. Rep., doi:10.1038/srep30571, 2016.

Wang, W., Wang, W. J., Li, J. S., Wu, H., Xu, C. and Liu, T.: The impact of sustained drought on vegetation ecosystem in southwest China based on remote sensing, in Procedia Environmental Sciences., 2010.

Werner, A. T. and Cannon, A. J.: Hydrologic extremes - An intercomparison of multiple gridded statistical downscaling methods, Hydrol. Earth Syst. Sci., doi:10.5194/hess-20-1483-2016, 2016.

Winston, H.A., Ruthi, L.J.: Evaluation of RADAP II severe-storm-detection algorithms. Bull. Am. Meteorol. Soc., 67(2), 145-150, doi.org/10.1175/1520-0477(1986)067<0145:EORISS>2.0.CO;2 1986.

Wu, J., Chen, X., Yao, H., Liu, Z. and Zhang, D.: Hydrological Drought Instantaneous Propagation Speed Based on the Variable Motion Relationship of Speed-Time Process, Water Resour. Res., doi:10.1029/2018WR023120, 2018.

Wu, X., Hao, Z., Hao, F. and Zhang, X.: Variations of compound precipitation and temperature extremes in China during 1961–2014, Sci. Total Environ., 663, 731–737, doi:10.1016/j.scitotenv.2019.01.366, 2019.

Wu, X., Hao, Z., Zhang, X., Li, C. and Hao, F.: Evaluation of severity changes of compound dry and hot events in China based on a multivariate multi-index approach, J. Hydrol., 583, 124580, doi:10.1016/j.jhydrol.2020.124580, 2020.

Xia, Y., Mocko, D. M., Wang, S., Pan, M., Kumar, S. V., and Peters-Lidard, C. D.: Comprehensive evaluation of the variable infiltration capacity (VIC) model in the North American Land Data Assimilation System. Journal of Hydrometeorology, 19(11), 1853-1879, 2018.

Xu, C., McDowell, N. G., Fisher, R. A., Wei, L., Sevanto, S., Christoffersen, B. O., Weng, E. and Middleton, R. S.: Increasing impacts of extreme droughts on vegetation productivity under climate change, Nat. Clim. Chang., 9(12), 948–953, doi:10.1038/s41558-019-0630-6, 2019.

Xu, K., Yang, D., Yang, H., Li, Z., Qin, Y. and Shen, Y.: Spatio-temporal variation of drought in China during 1961-2012: A climatic perspective, J. Hydrol., doi:10.1016/j.jhydrol.2014.09.047, 2015.

Yang, Y., Bai, L., Wang, B., Wu, J. and Fu, S.: Reliability of the global climate models during 1961–1999 in arid and semiarid regions of China, Sci. Total Environ., doi:10.1016/j.scitotenv.2019.02.188, 2019.

Yeo, I. N. K. and Johnson, R. A.: A new family of power transformations to improve normality or symmetry, Biometrika, 87(4), 954–959, doi:10.1093/biomet/87.4.954, 2000.

Yu, H., Zhang, Q., Xu, C. Y., Du, J., Sun, P. and Hu, P.: Modified Palmer Drought Severity Index: Model improvement and application, Environ. Int., 130(January), 104951, doi:10.1016/j.envint.2019.104951, 2019.

~~Vogel, M. M., Zscheischler, J. and Seneviratne, S. I.: Varying soil moisture-atmosphere feedbacks explain divergent temperature extremes and precipitation projections in central Europe, Earth Syst. Dyn., doi:10.5194/esd-9-1107-2018, 2018.~~

Yuan, X., Wang, L., Wu, P., Ji, P., Sheffield, J. and Zhang, M.: Anthropogenic shift towards higher risk of flash drought over China, Nat. Commun., doi:10.1038/s41467-019-12692-7, 2019.

~~Zhang, Q., Li, Q., Singh, V. P., Shi, P., Huang, Q. and Sun, P.: Nonparametric Integrated Agrometeorological Drought Monitoring: Model Development and Application, J. Geophys. Res. Atmos., 123(1), 73–88, doi:10.1002/2017JD027448, 2018.~~

Zhang, W. J., Lu, Q. F., Gao, Z. Q. and Peng, J.: Response of remotely sensed normalized difference water deviation index to the 2006 drought of eastern Sichuan Basin, Sci. China, Ser. D Earth Sci., 51(5), 748–758, doi:10.1007/s11430-008-0037-0, 2008.

Zhang, Y., You, Q., Chen, C. and Li, X.: Flash droughts in a typical humid and subtropical basin: A case study in the Gan River Basin, China, J. Hydrol., 551, 162–176, doi:10.1016/j.jhydrol.2017.05.044, 2017.

Zhang, Y., You, Q., Mao, G., Chen, C. and Ye, Z.: Short-term concurrent drought and heatwave frequency with 1.5 and 2.0 °C global warming in humid subtropical basins: a case study in the Gan River Basin, China, Clim. Dyn., 52(7–8), 4621–4641, doi:10.1007/s00382-018-4398-6, 2019.

Zhong, R., Chen, X., Lai, C., Wang, Z., Lian, Y., Yu, H. and Wu, X.: Drought monitoring utility of satellite-based precipitation products across mainland China, J. Hydrol., 568(June 2018), 343–359, doi: 10.1016/j.jhydrol.2018.10.072, 2019a.

Zhong, R., Zhao, T., He, Y. and Chen, X.: Hydropower change of the water tower of

Asia in 21st century: A case of the Lancang River hydropower base, upper Mekong, Energy, 179, 685–696, doi:10.1016/j.energy.2019.05.059, 2019b.

Zscheischler, J., Michalak, A. M., Schwalm, C., Mahecha, M. D. and Zeng, N.: Impact of large-scale climate extremes on biospheric carbon fluxes: An intercomparison based on MsTMIP data, Global Biogeochem. Cycles, 28(6), 585–600, doi:10.1002/2014GB004826, 2014.

Zscheischler, J., Orth, R. and Seneviratne, S. I.: Bivariate return periods of temperature and precipitation explain a large fraction of European crop yields, Biogeosciences, doi:10.5194/bg-14-3309-2017, 2017a.

Zscheischler, J. and Seneviratne, S. I.: Dependence of drivers affects risks associated with compound events, Sci. Adv., 3(6), 1–11, doi:10.1126/sciadv.1700263, 2017b.

Zscheischler, J., Westra, S., Van Den Hurk, B. J. J. M., Seneviratne, S. I., Ward, P. J., Pitman, A., Aghakouchak, A., Bresch, D. N., Leonard, M., Wahl, T. and Zhang, X.: Future climate risk from compound events, Nat. Clim. Chang., 8(6), 469–477, doi:10.1038/s41558-018-0156-3, 2018.

Zscheischler, J., Martius, O., Westra, S., Bevacqua, E. and Raymond, C.: A typology of compound weather and climate events, Nat. Rev. Earth Environ., doi: https://doi.org/10.1038/s43017-020-0060-z, 2020.

Zhou, J., Wu, Z., He, H., Wang, F., Xu, Z., and Wu, X.: Regional assimilation of in situ observed soil moisture into the VIC model considering spatial variability. Hydrological Sciences Journal, 64(16), 1982-1996, 2019

Table

Table 1 Categories of compound dry and hot conditions based on SCDHI.

Category	Dry and hot condition	SCDHI
~~G~~Grade 0~~$_0$~~	Abnormal	(-0.80, -0.50]
Grade 0~~G_1~~	Light	(-1.30, -0.80]
Grade 0~~G_2~~	Moderate	(-1.60, -1.30]
Grade 0~~G_3~~	Heavy	(-2.0, -1.60]
Grade 0~~G_4~~	Extreme	≤ -2

Figure

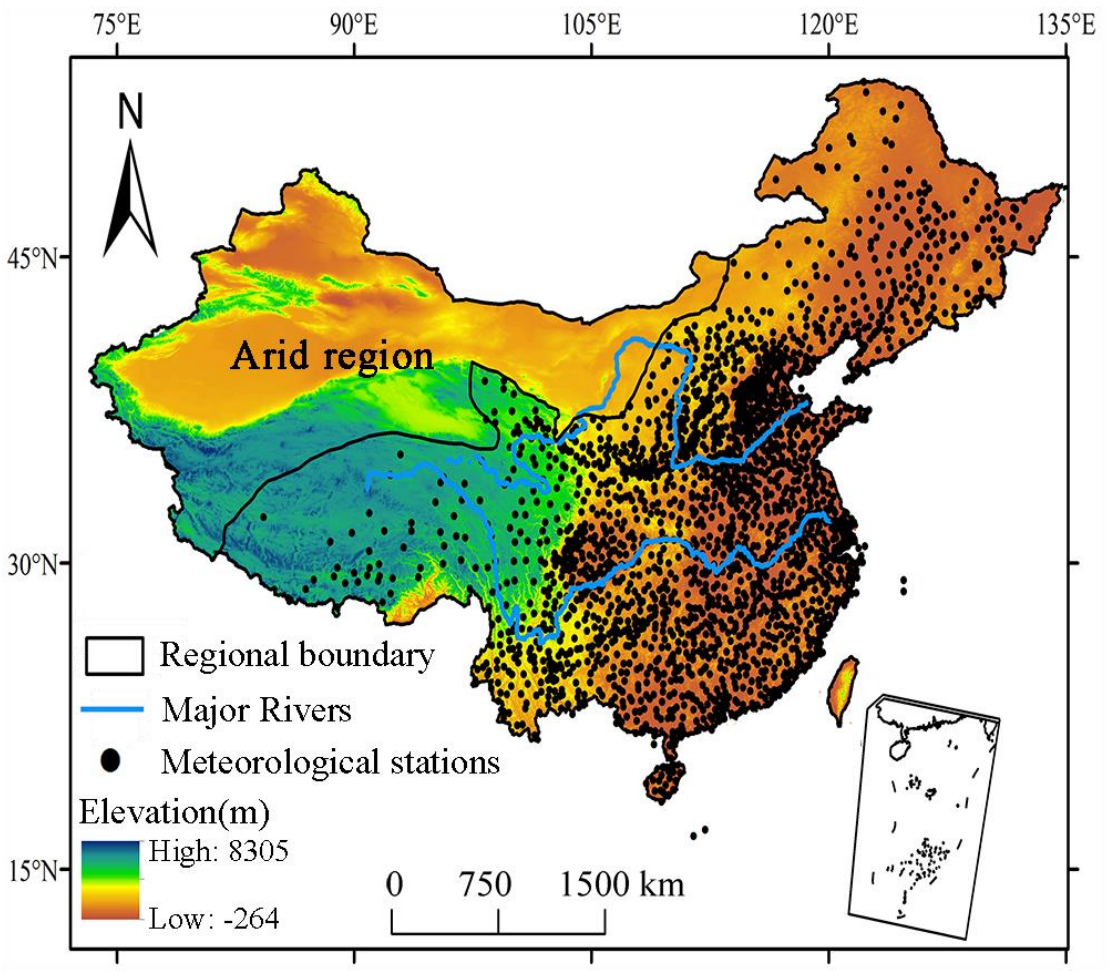

Figure 1 Geographical position of China and local of meteorological stations.

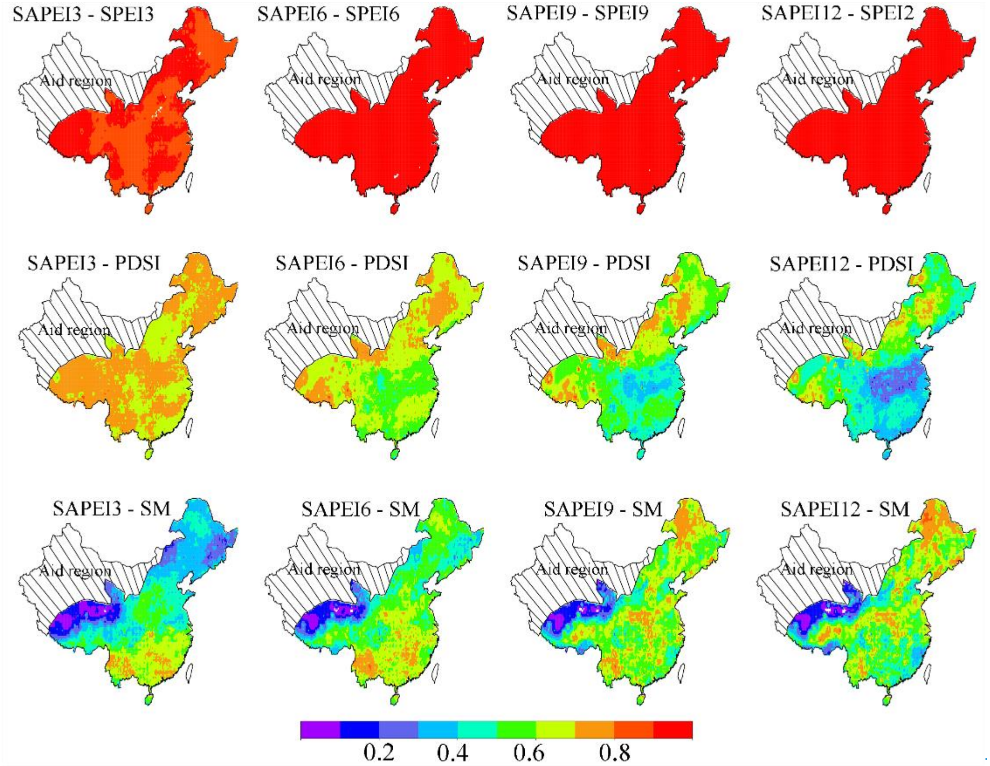

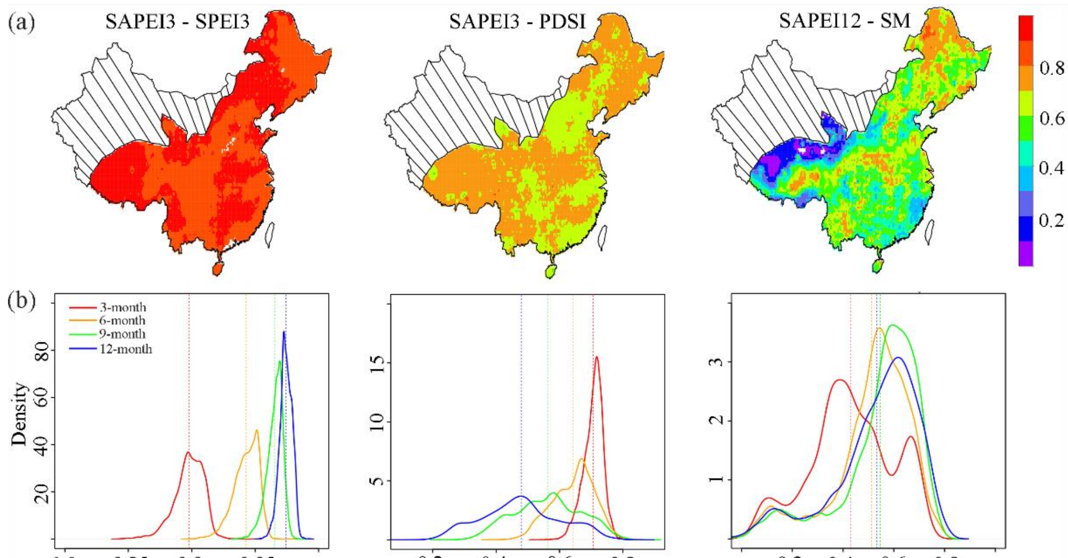

Figure 2 (a) The spatial pattern of the correlations between monthly SAPEI and SPEI/PDSI, and between daily SAPEI and soil moisture (SM), and (b) The density plot for the correlations. ~~.~~The monthly SAPEI is computed by averaging the daily values in each month.

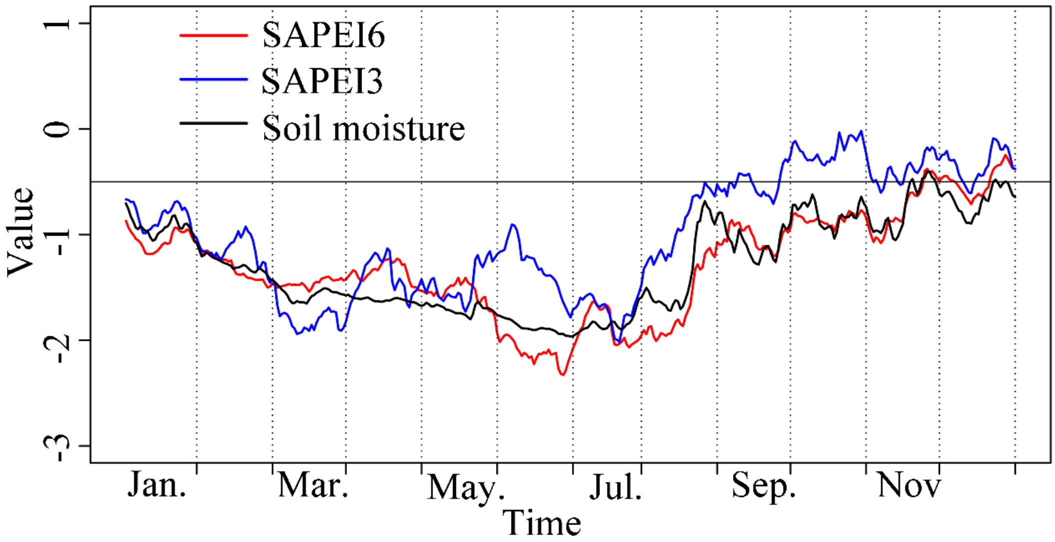

Figure 3 SAPEI ~~(3- and 6-month)~~ and soil moisture series during the 2009/2010 drought event over the southwest China. The series were spatially average merged series. The value of solid black line is at -0.5, indicating the distinction between drought and non-drought.

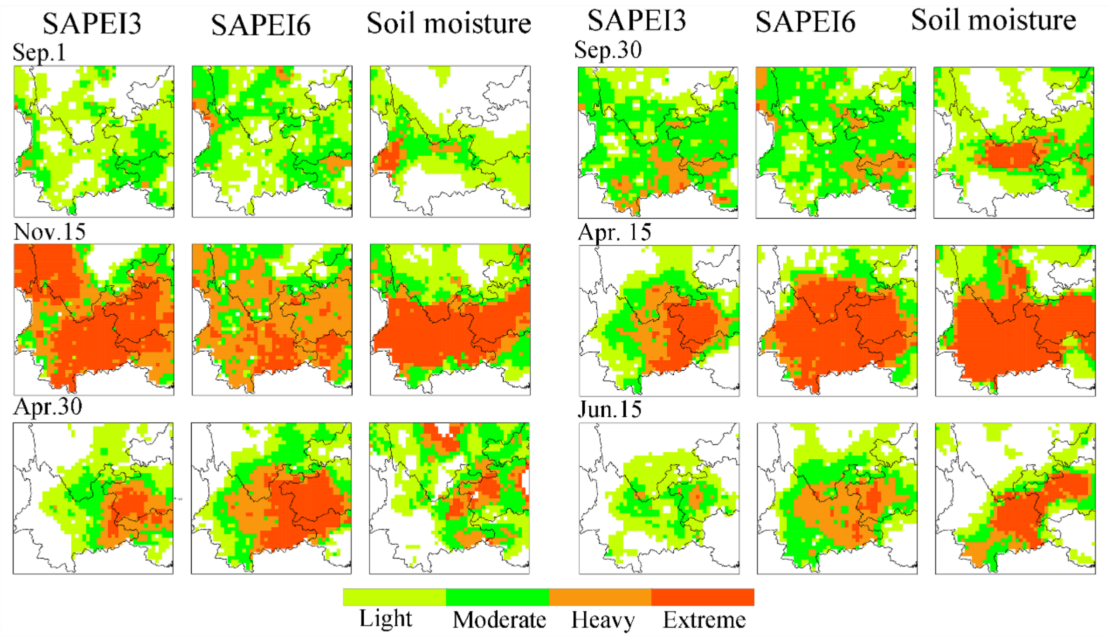

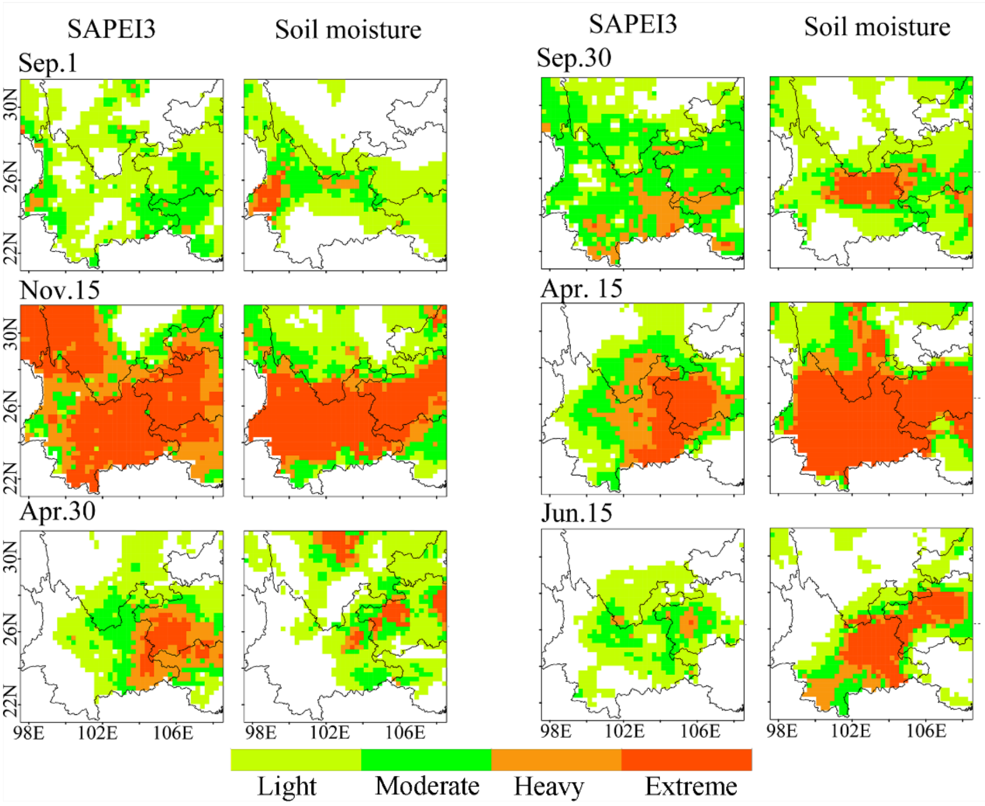

Figure 4 Daily evolutions of the 2009/2010 drought event over the southwest China monitored by 3-~~and 6-~~month SAPEI and soil moisture.

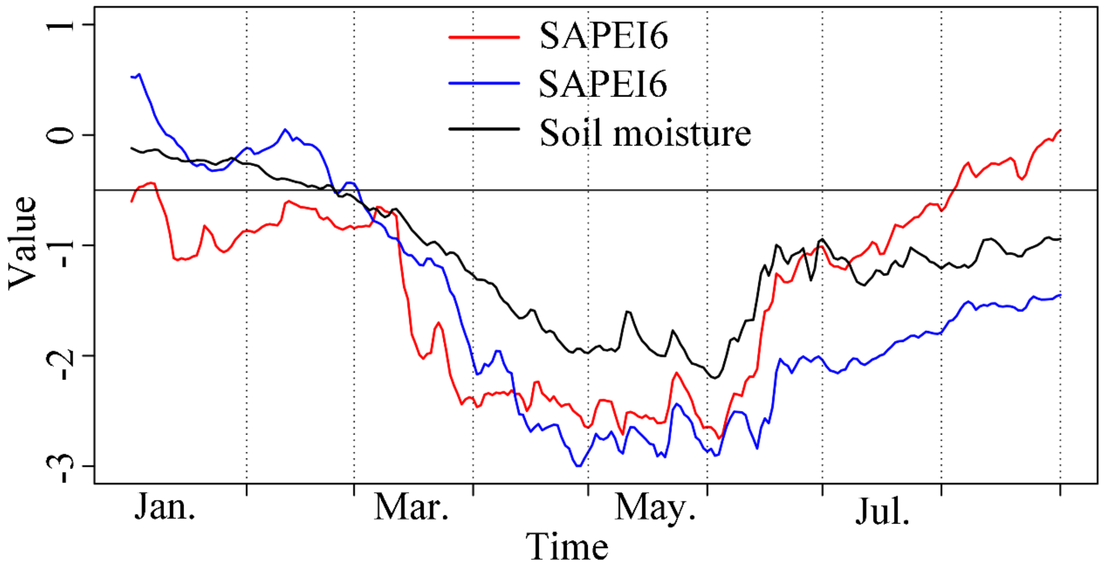

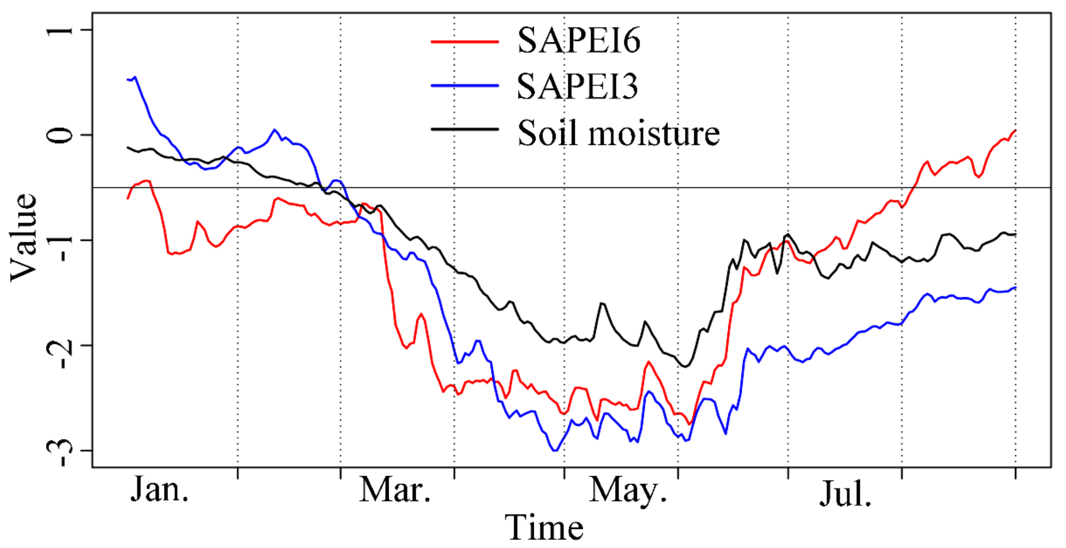

Figure 5 SAPEI (3- and 6-month) and soil moisture series during the 2011 drought event over the middle and lower reaches of the Yangtze River. The series were spatially average merged series. The value of solid black line is at -0.5, indicating the distinction between drought and non-drought.

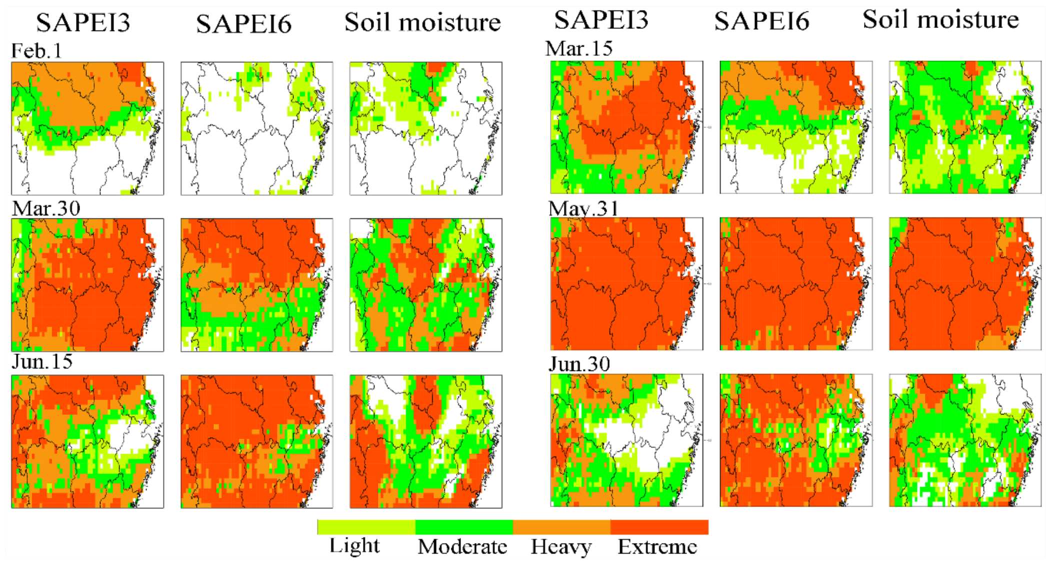

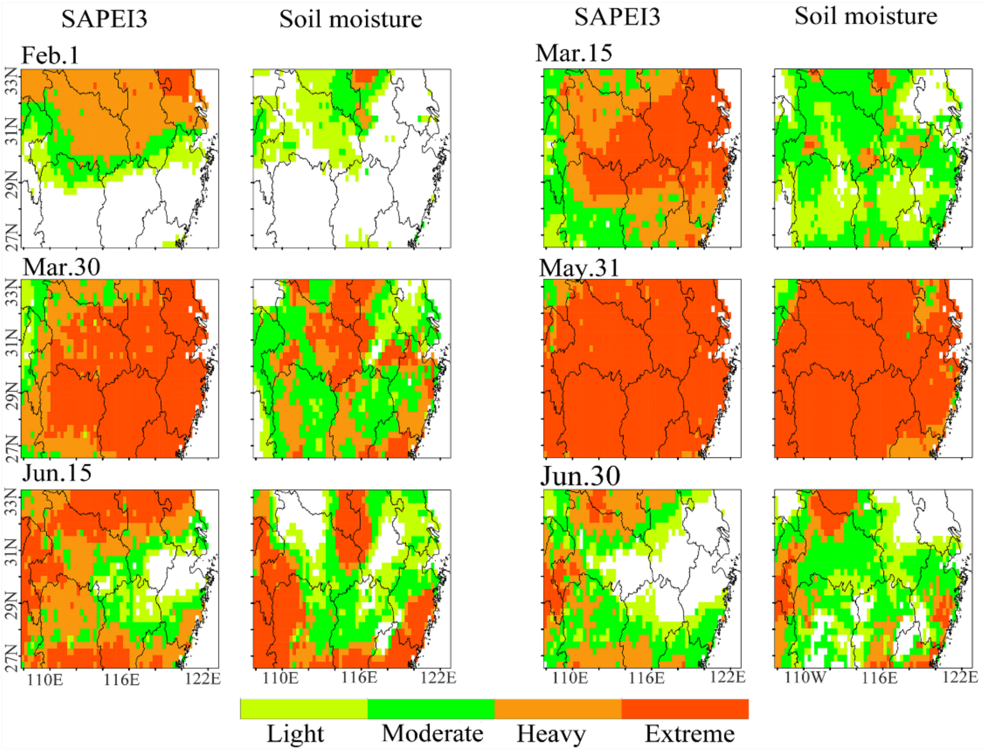

Figure 6 Daily evolutions of the 2011 drought event over the middle and lower reaches of the Yangtze River monitored by 3-~~ and 6~~ -month SAPEI and soil moisture.

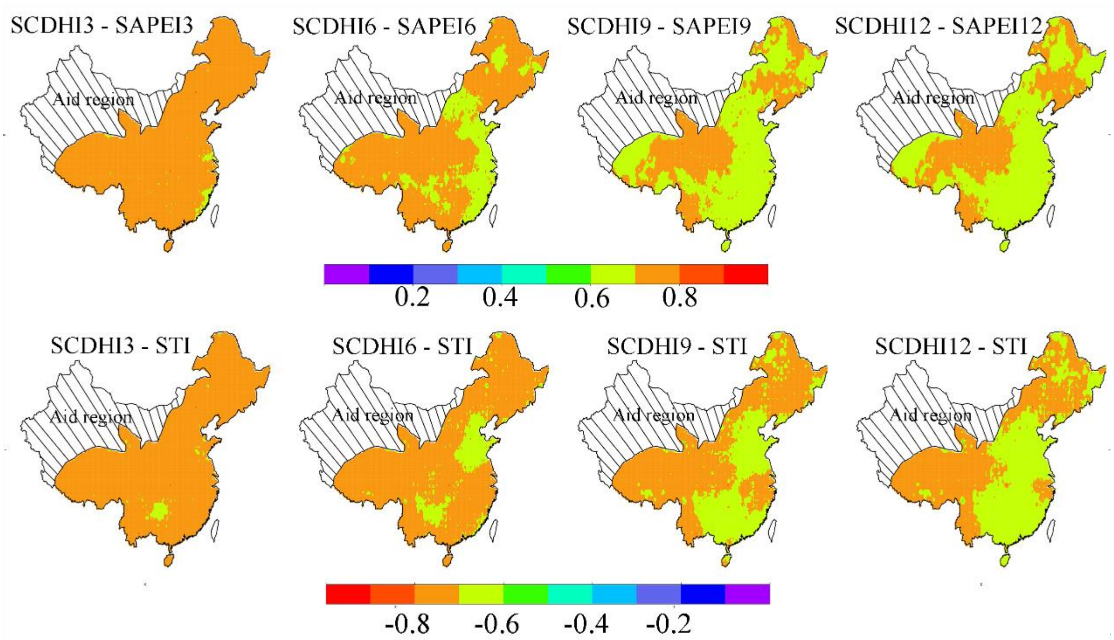

~~Figure 7 The spatial pattern of the correlations between SCDHI and SAPEI/STI at daily scale from 1961 to 2018.~~

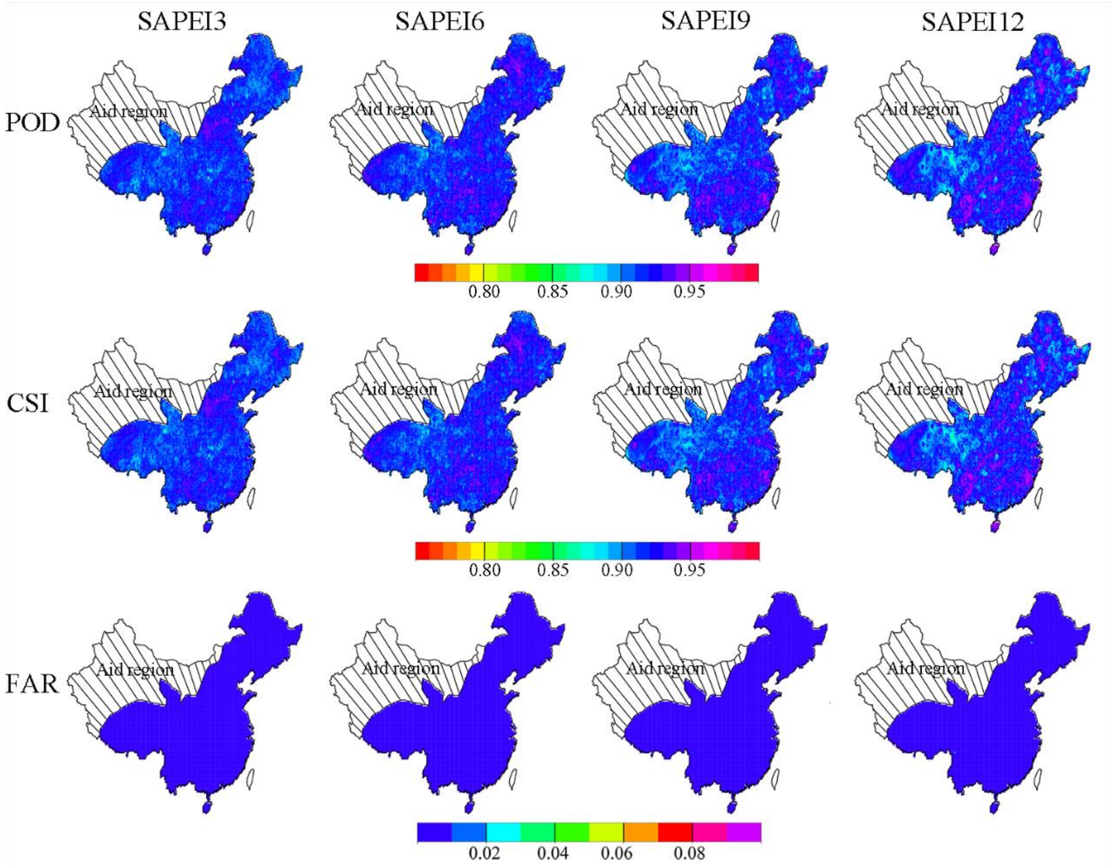

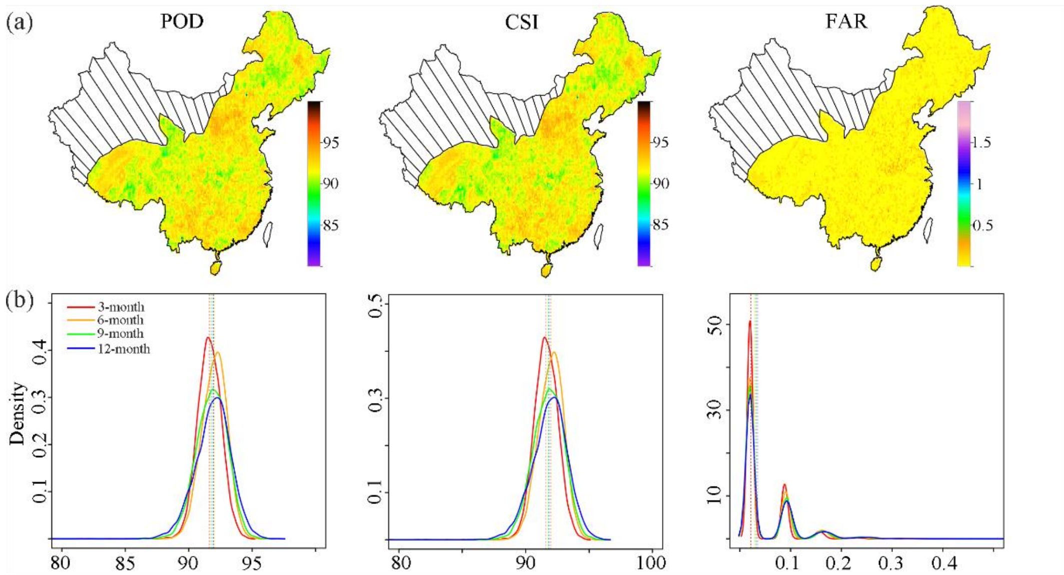

Figure ~~8~~ 7 (a) The spatial pattern of probability of detection (POD)~~POD~~ (%), ~~FAR, and~~ critical success index (CSI)~~CSI~~ (%), and false alarm ratio (FAR) for 3-month SCDHI ~~at 3-, 6-, 9- and 12-month time scales~~ from 1961 to 2018, and (b) Density plot for POD, FAR, and CSI for 3-, 6-, 9-, 12-month SCDHI from 1961 to 2018.

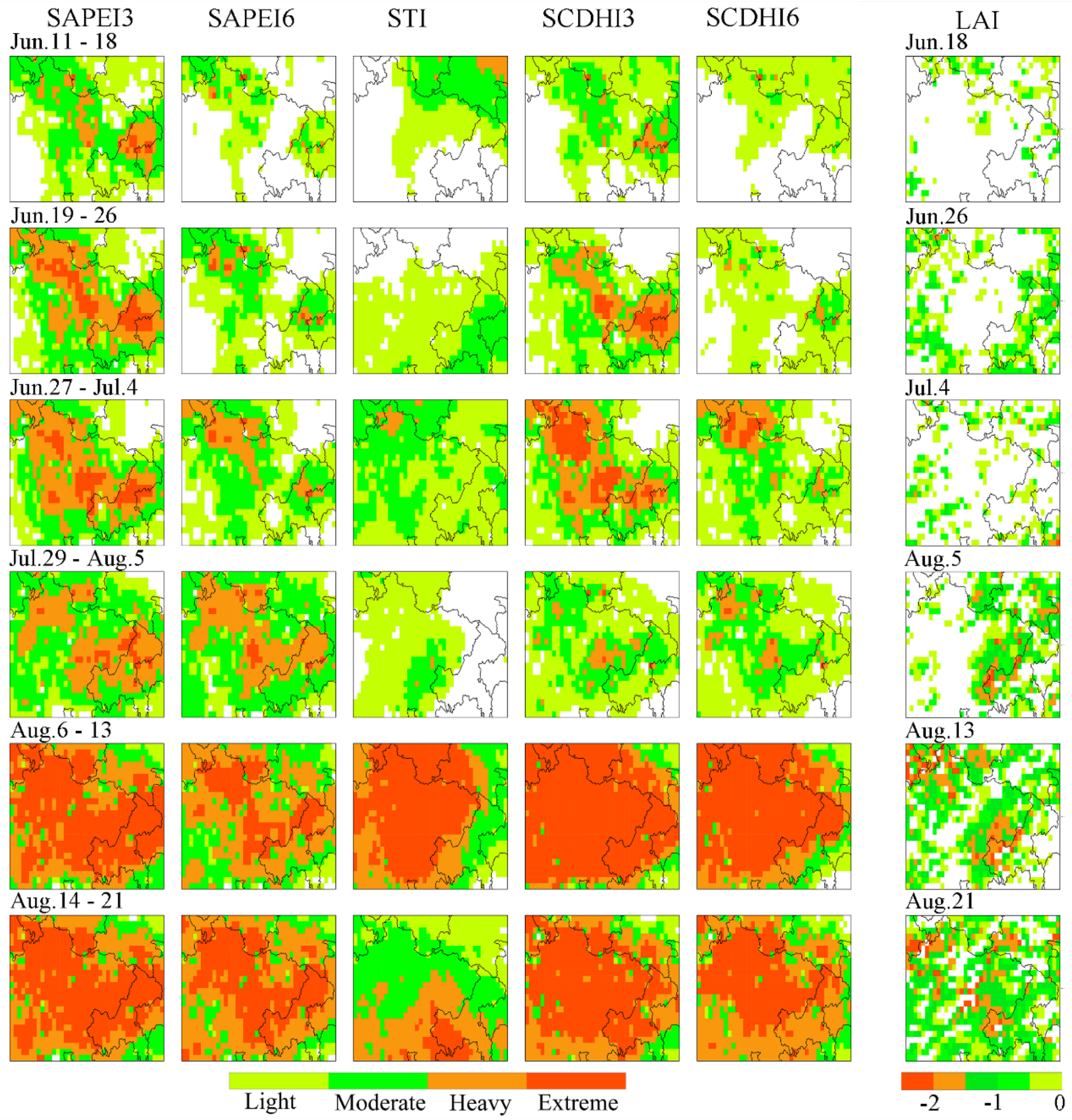
SAPEI3
SAPEI6
STI
SCDHI3
SCDHI6
LAI
Jun.11 - 18
Jun.18
Jun.19 - 26
Jun.26
Jun.27 - Jul.4
Jul.4
Jul.29 - Aug.5
Aug.5
Aug.6 - 13
Aug.13
Aug.14 - 21
Aug.21
Light
Moderate
Heavy
Extreme
-2
-1
0

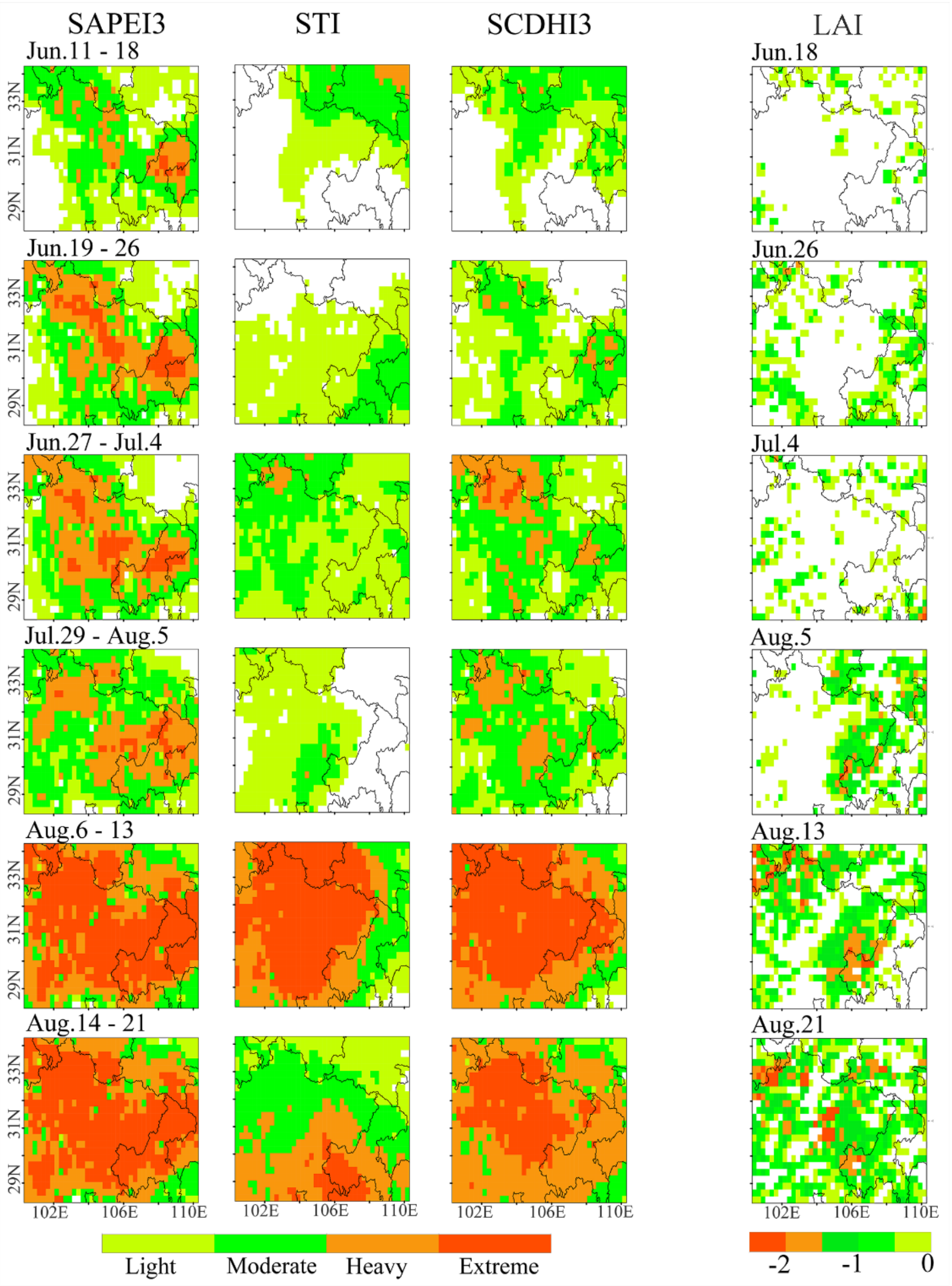

Figure ~~9~~8~~.~~ The spatial evolutions of the compound dry and hot event over the Sichuan-Chongqing region in 2006 and its impact on vegetation.

1009

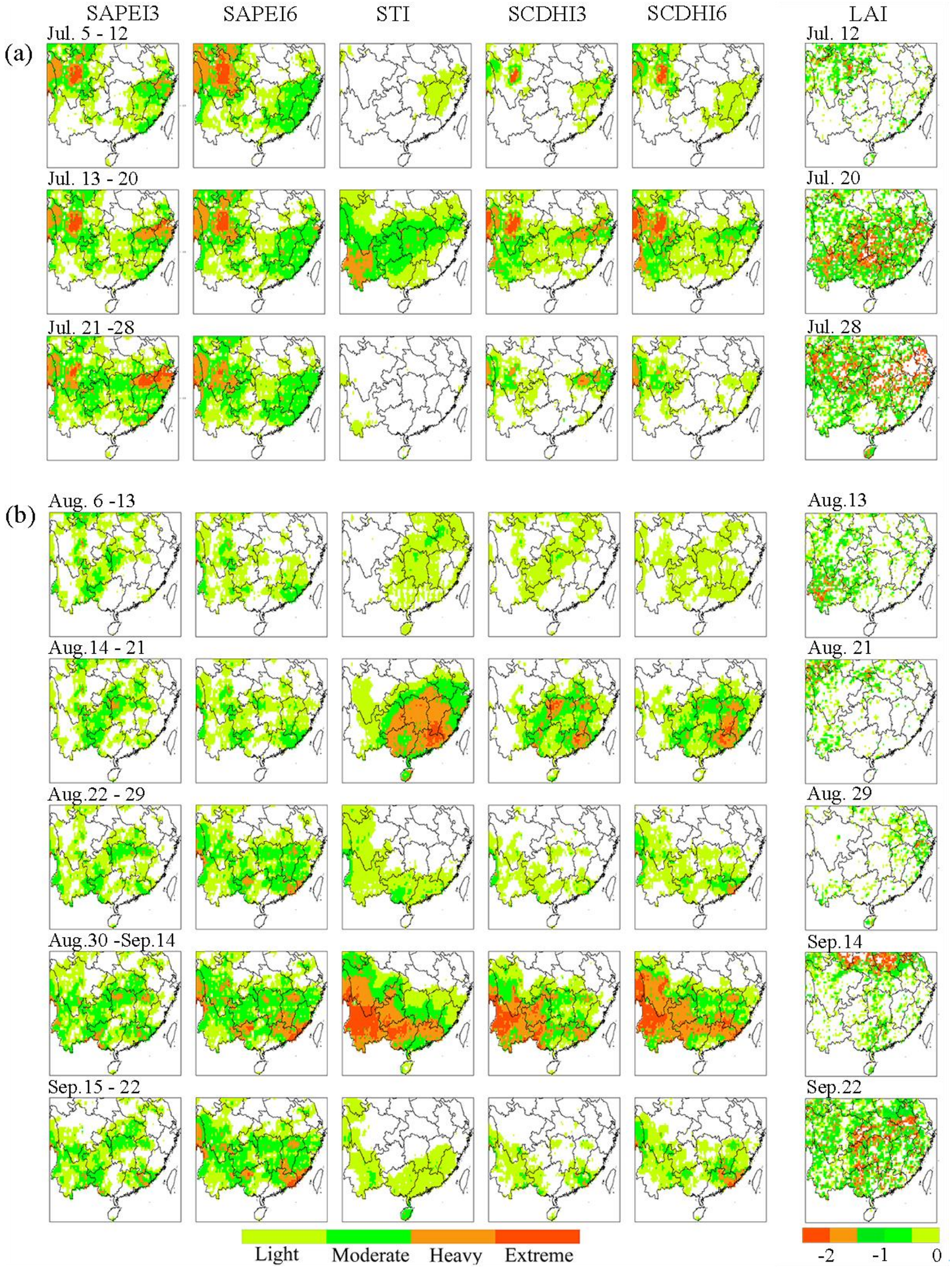

SAPEI3
SAPEI6
STI
SCDHI3
SCDHI6
LAI
(a)
Jul. 5 - 12
Jul. 12
Jul. 13 - 20
Jul. 20
Jul. 21 -28
Jul. 28
(b)
Aug. 6 -13
Aug.13
Aug.14 - 21
Aug. 21
Aug.22 - 29
Aug. 29
Aug.30 -Sep.14
Sep.14
Sep.15 - 22
Sep.22
Light
Moderate
Heavy
Extreme
-2
-1
0

1010

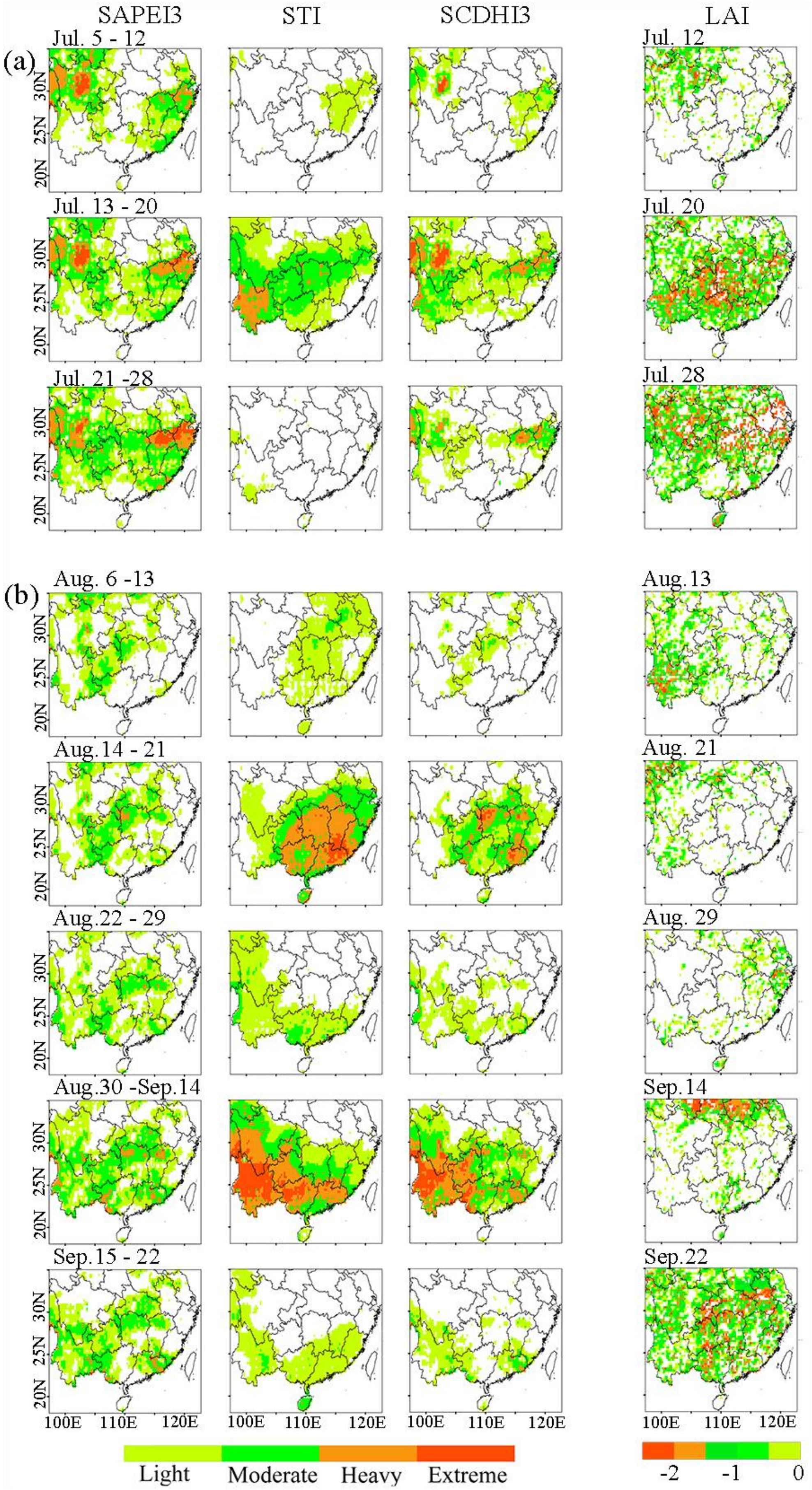
SAPEI3
STI
SCDHI3
LAI
(a)
Jul. 5 - 12
Jul. 12
Jul. 13 - 20
Jul. 20
Jul. 21 -28
Jul. 28
(b)
Aug. 6 -13
Aug.13
Aug.14 - 21
Aug. 21
Aug.22 - 29
Aug. 29
Aug.30 -Sep.14
Sep.14
Sep.15 - 22
Sep.22
30N
25N
20N
100E
110E
120E
Light
Moderate
Heavy
Extreme
-2
-1
0

Figure ~~10~~ 9 The spatial evolutions of the compound dry and hot event over the southern China in 2009 and its impact on vegetation.

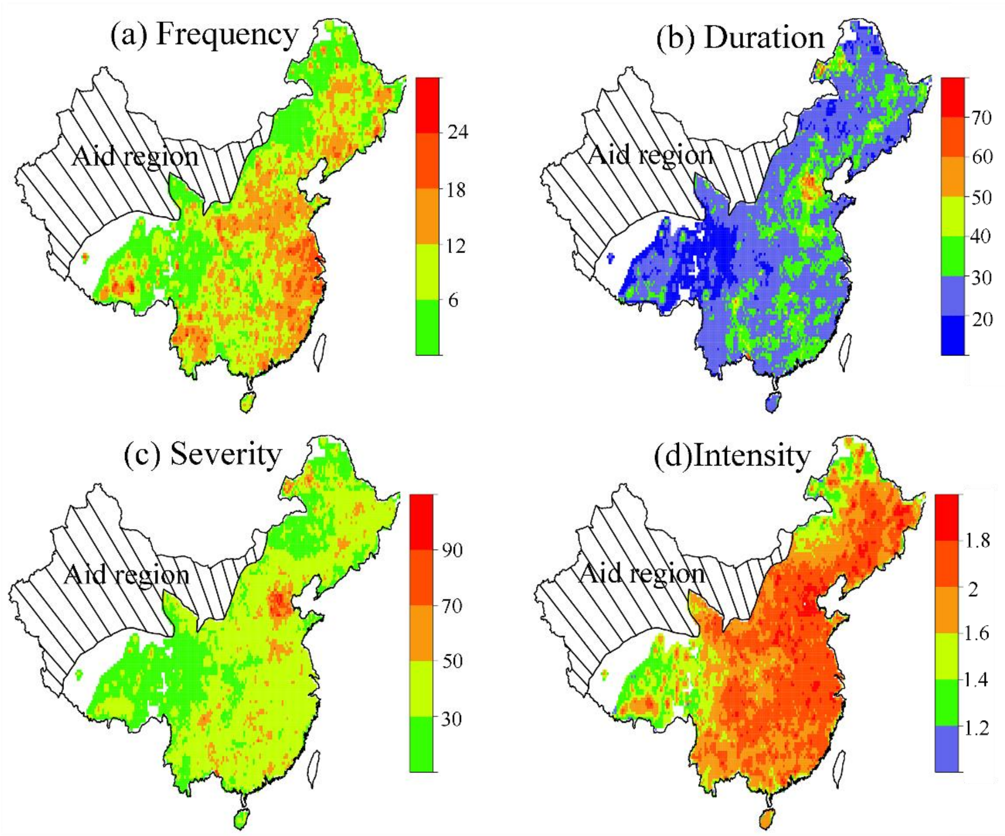

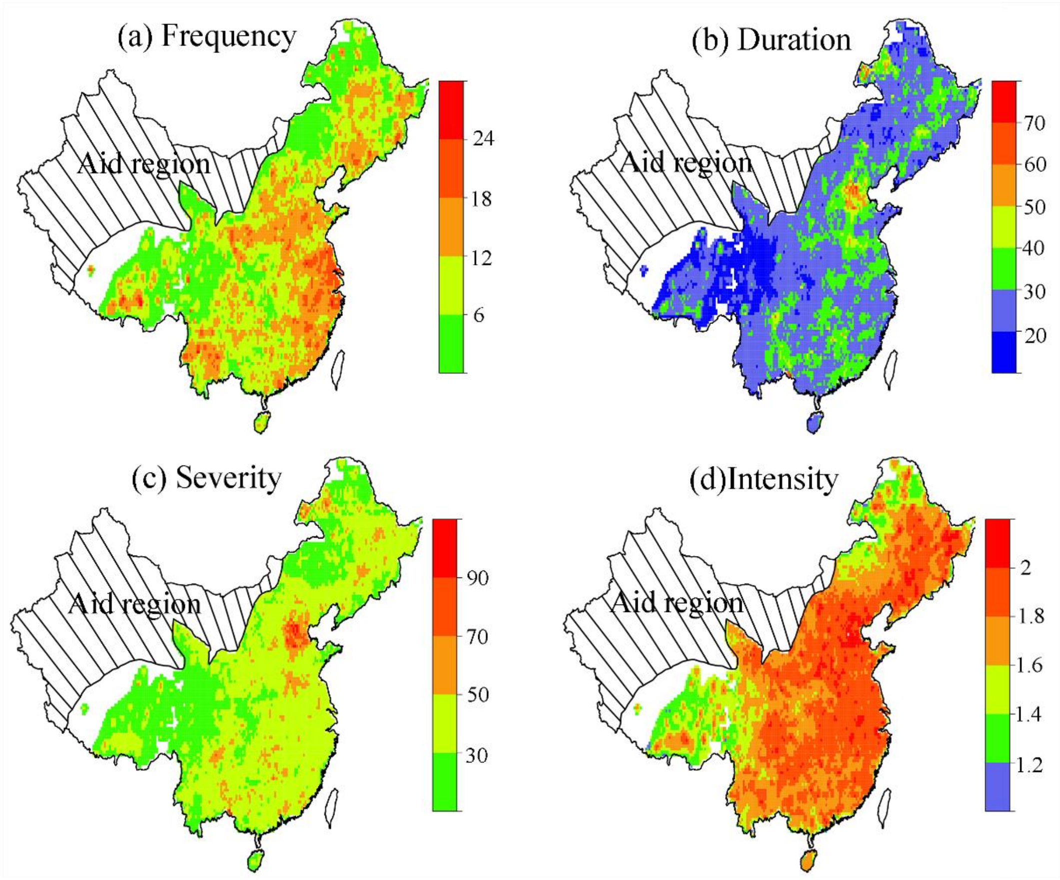

Figure ~~11~~ 10 The spatial pattern of the characteristics of the compound dry and hot event in China from 1961 to 2018.

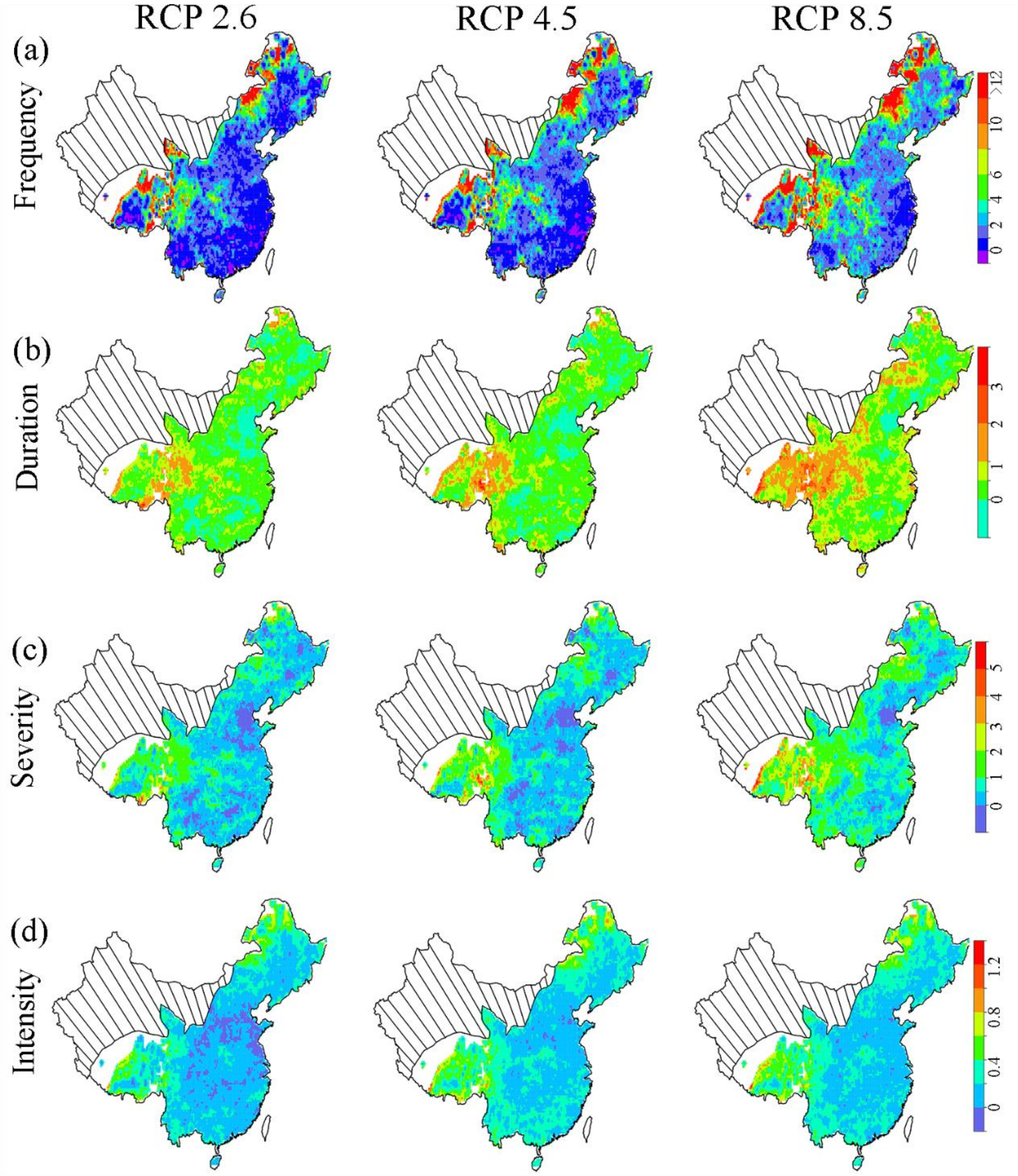

Figure ~~12~~ 11 Future changes in characteristics of the compound dry and hot events under the RCP 2.6, RCP4.5 and RCP8.5 scenarios. The change values were the ratio of the future value to the reference values. Reference period: 1961-2018, and future period: 2050-2100.

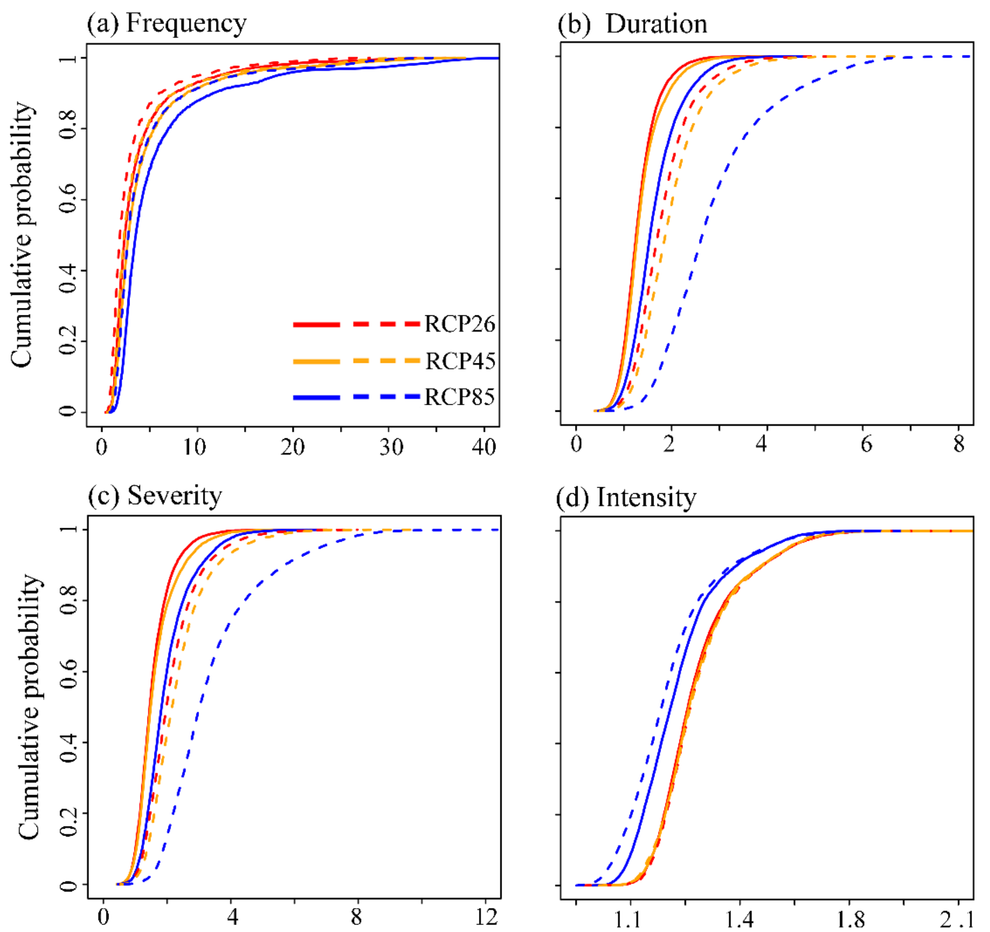

Figure 12 Cumulative probability of future changes (multiple) in of the compound dry-hot event characteristics. The dash lines indicate future characteristics changes only considered temperature change, while solid lines represent the future changes driven by all variable variation.

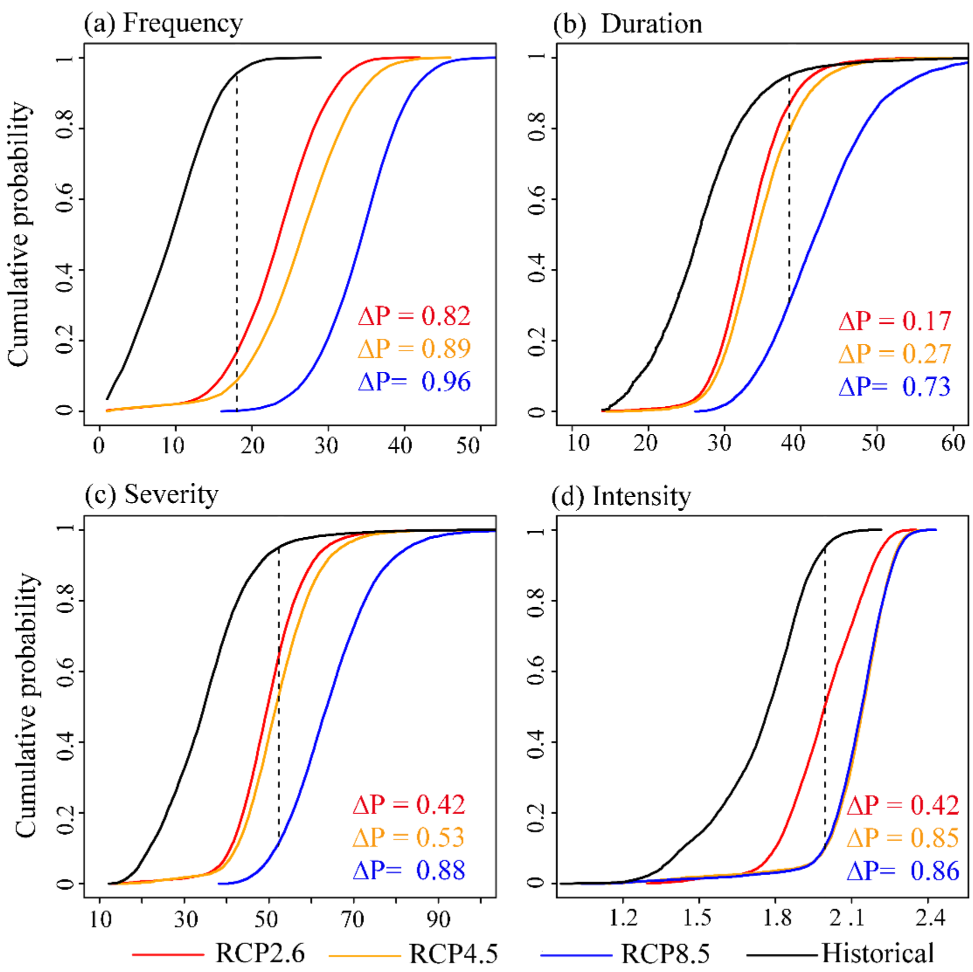

~~Figure 13 Cumulative probability functions of characteristics of the compound drought and hot events in historical and future period. The vertical lines denote the probability of the 95^th^ percentile value during the historical period. Δ*P* denotes the changes in the probability of the 95^th^ percentile value between the historical period and the future period. Reference period: 1961-2018, and future period: 2050-2100. The red, orange, and blue fonts refer to the change values under RCP 2.6, 4.5 and 8.5 scenario, respectively.~~